RESTRICTED

Copy No. 206

RM No. L8J07

NACA RM No. L8J07

NACA

RESEARCH MEMORANDUM

THE EFFECT OF NEGATIVE DIHEDRAL, TIP DROOP, AND WING-TIP SHAPE ON THE LOW-SPEED AERODYNAMIC CHARACTERISTICS OF A COMPLETE MODEL HAVING A 45° SWEPTBACK WING

By

M. Leroy Spearman and Robert E. Becht

Langley Aeronautical Laboratory
Langley Field, Va.

NATIONAL ADVISORY COMMITTEE
FOR AERONAUTICS

WASHINGTON

December 6, 1948

RESTRICTED

NATIONAL ADVISORY COMMITTEE FOR AERONAUTICS

RESEARCH MEMORANDUM

THE EFFECT OF NEGATIVE DIHEDRAL, TIP DROOP, AND WING-TIP SHAPE ON THE LOW-SPEED AERODYNAMIC CHARACTERISTICS OF A COMPLETE MODEL HAVING A 45° SWEPTBACK WING

By M. Leroy Spearman and Robert E. Becht

SUMMARY

An investigation has been conducted in the Langley 300 MPH 7- by 10-foot tunnel to determine the effect of negative dihedral, tip droop, and wing-tip shape on the low-speed aerodynamic characteristics of a complete model having a 45° sweptback wing. Longitudinal and lateral stability characteristics were obtained for the model with and without tail surfaces.

The results of the investigation indicated that the effective-dihedral parameter C_{l_ψ} was reduced by the use of either negative geometric dihedral in the wing, wing-tip droop, or by changes in the wing-tip plan form and cross section.

Because the wing tips were deflected about an axis in the wing approximately normal to the wing midchord line, they also increased the maximum lift coefficient and were effective as a lateral-control device when operated differentially from an initial position of zero deflection.

INTRODUCTION

Previous investigations have shown that undesirable stability and control characteristics may be encountered at moderate and high lift coefficients with wings having large angles of sweepback. One of the more objectionable characteristics is that of high values of effective dihedral in the higher lift range.

One method of minimizing this effect requires the use of negative geometric dihedral. It was shown in reference 1 that changes in geometric dihedral angles from 0° to -10° resulted in reductions in the effective dihedral throughout the lift range. The results of the investigation reported in reference 2 indicated that the effective

dihedral as well as the rate of change of effective dihedral with lift coefficient could be reduced by drooping the tips of a sweptback wing.

The actual shape of the wing tips might be considered as another influencing factor inasmuch as changes in the tip shape affect the span load distribution.

The present investigation was undertaken in order to determine to what extent independent changes of wing geometric dihedral, wing-tip droop, and changes in wing-tip shape would affect the aerodynamic characteristics of a complete model having a 45° sweptback wing.

Another problem arising from the use of large angles of sweepback is that of lateral control. Among the lateral-control devices proposed for high-speed airplanes having sweptback wings are wing-tip ailerons hinged about an axis normal to the leading edge so that the ailerons, when deflected, are approximately normal to the spanwise flow on the wing. Inasmuch as the tips herein discussed were drooped about an axis normal to the 0.487 chord line, it appeared desirable to investigate their utility as a lateral-control device. Accordingly, some tests were made through the lift-coefficient range with the right wing tip deflected while the left wing tip was held at zero deflection.

COEFFICIENTS AND SYMBOLS

The results of the tests are presented as standard NACA coefficients of forces and moments. All forces and moments are presented for the stability axes shown in figure 1 with the reference center of gravity at the 25 percent mean aerodynamic chord as shown in figure 2.

The coefficients and symbols are defined as follows:

C_L lift coefficient (Lift/qS where lift = -Z)

C_X longitudinal-force coefficient (X/qS)

C_Y lateral-force coefficient (Y/qS)

C_l rolling-moment coefficient (L/qSb)

C_m pitching-moment coefficient ($M/qS\bar{c}$)

C_n yawing-moment coefficient (N/qSb)

Z force along Z-axis, pounds

X force along X-axis, pounds

Y	force along Y-axis, pounds
L	rolling moment about X-axis, pound-feet
M	pitching moment about Y-axis, pound-feet
N	yawing moment about Z-axis, pound-feet
q	free-stream dynamic pressure, pounds per square foot $\left(\rho V^2/2\right)$
S	wing area, square feet
b	wing span, feet
$\bar{c}$	wing mean aerodynamic chord (M.A.C.), feet $\left(\frac{2}{S}\int_0^{b/2} c^2\, dy\right)$
c	airfoil section chord, feet
ρ	mass density of air, slugs per cubic foot
V	air velocity, feet per second
y	distance along wing span, feet
A	aspect ratio $\left(b^2/S\right)$
c.g.	center of gravity
α	angle of attack of fuselage center line, degrees
ψ	angle of yaw, degrees
i_t	angle of stabilizer with respect to fuselage center line, degrees
Γ	geometric dihedral angle, degrees
δ_T	tip deflection angle, degrees
C_{l_ψ}	effective dihedral parameter, rate of change of rolling-moment coefficient with angle of yaw, per degree $\left(\frac{\partial C_l}{\partial \psi}\right)$
C_{n_ψ}	directional-stability parameter, rate of change of yawing-moment coefficient with angle of yaw, per degree $\left(\frac{\partial C_n}{\partial \psi}\right)$

C_{Y_ψ} lateral-force parameter, rate of change of lateral-force coefficient with angle of yaw, per degree $\left(\frac{\partial C_Y}{\partial \psi}\right)$

$C_{l_{\psi C_L}}$ rate of change of effective-dihedral parameter with lift coefficient $\left(\frac{\partial C_{l_\psi}}{\partial C_L}\right)$

$C_{l_{\psi_\Gamma}}$ rate of change of effective-dihedral parameter with geometric dihedral angle, per degree $\left(\frac{\partial C_{l_\psi}}{\partial \Gamma_w}\right)$

$C_{l_{\delta_T}}$ rate of change of rolling-moment coefficient with tip deflection angle, per degree $\left(\frac{\partial C_l}{\partial \delta_T}\right)$

Subscripts:

W	wing
T	tip
R	right
L	left

MODEL AND APPARATUS

A three-view drawing of the model is presented in figure 2 and the geometric characteristics of the model are given in table I. The model mounted for testing in the Langley 300 MPH 7- by 10-foot tunnel is shown in figure 3.

The model was designed so that the wing could be set at geometric dihedral angles of 0° or -10°. (See fig. 2.)

The model with the wing having 0° geometric dihedral was also tested with the tip portion of the wing (5 percent of one wing panel area) deflected about an axis in the wing plane normal to 0.487c line as shown in figure 4. The ground clearance was the same with 45° tip droop as with -10° geometric dihedral. To determine the rolling effectiveness of the drooped tip as an aileron, some tests were made with only the right tip deflected.

The model was also tested with different tip shapes on the wing with 0° geometric dihedral by utilizing five interchangeable pairs of wing tips so designed that the wing aspect ratio remained nearly constant for each tip. The various wing plan forms are shown in figure 5. All of the tips were faired semicircular with the exception of tip 1a which was geometrically the same as tip 1 but was unfaired.

Hereinafter, the model having 0° geometric dihedral, 0° tip droop, and equipped with tip 1 shall be referred to as the basic model.

TESTS

Test Condition

All tests were made at a dynamic pressure of 30 pounds per square foot. The test Reynolds number based on a mean aerodynamic chord of 17.57 inches for the basic model was 1,483,000 and the test Mach number was 0.14. The turbulence factor for the tunnel is not known but is believed to be approximately 1 because of the high tunnel contraction ratio (14:1).

Test Procedure

Included in the investigation were some tests made to determine the effect of the tail unit on the aerodynamic characteristics. For these tests the aft portion of the fuselage, including the vertical and horizontal tails, was removed and replaced by a dummy fuselage without tail surfaces. For the complete model, pitch tests were made with two stabilizer settings and with the tail off. In this case only the horizontal tail was removed.

The pitch tests were made through an angle-of-attack range from -4° to 20°. The lateral-stability parameters were determined from pitch tests made with the model yawed 5° and -5°.

Corrections

Tare corrections were considered negligible and were not applied. Jet-boundary corrections were computed by the methods of reference 3. The correction formulas given in reference 3 are for straight wings, but an unpublished analysis indicates that little error is incurred when the same corrections are applied to swept wings up to 45° sweep. Corrections were applied as follows:

$$\alpha = \alpha_M + 0.845C_{L_M}$$

$$C_x = C_{X_M} - 0.0129C_{L_M}^2$$

$$C_m = C_{m_M} + 0.0175C_{L_M} \qquad \text{(for tail on)}$$

where the subscript M denotes measured values.

All forces and moments were corrected for blocking by the method given in reference 4. An increment in longitudinal-force coefficient has been applied to account for the horizontal buoyancy occasioned by the longitudinal pressure gradient in the tunnel.

RESULTS AND DISCUSSION

A table of figures presenting the results follows:

Lift and Drag Characteristics

Effect of negative geometric dihedral.- The use of -10° geometric dihedral in the wing resulted in a slight decrease in the lift-curve slope C_{L_α} from that of the basic model (figs. 6 and 7(a)) in accordance with the theoretical relationship (from reference 1)

$$\left(C_{L_\alpha}\right)_{\Gamma_W} = \left(C_{L_\alpha}\right)_{\Gamma_W=0} \cos^2\Gamma_W$$

The maximum lift coefficient was less for the model with negative dihedral since the lift coefficients were based on the original wing area and not the projected wing area which decreases with dihedral. The angle of attack for maximum lift, however, was higher for the model with negative dihedral than for the basic model because the angle of attack measured in a plane normal to the wing surface determines the stall and this angle decreases with dihedral. Similar effects were obtained from the investigation reported in reference 1.

Negative geometric dihedral produced little effect on the drag at low lift coefficients. At the higher lift coefficients, however, the drag was higher for the model with -10° dihedral than for the basic

model, since at the same lift coefficient the model with -10° dihedral had the higher angle of attack.

Effect of tip droop.- Drooping the wing tips 45° resulted in no change in C_{L_α} but did effect a change in the angle of zero lift and produced an increase of about 0.15 in the maximum lift coefficient in the manner characteristic of a trailing-edge flap (figs. 6 and 8(a)). The effect would be anticipated inasmuch as the tips are deflected about an axis approximately normal to the wing midchord line and thus act partially as a trailing-edge flap.

Drooping the wing tips also resulted in an increase in drag coefficient, but the sinking speed at maximum lift was the same as for the basic model.

Effect of tip shape.- Variation of the wing-tip shape had no noticeable effect on C_{L_α}, the maximum lift, or the drag (figs. 6 and 9).

Pitching-Moment Characteristics

The variation of the pitching-moment coefficient with lift coefficient for the basic model (fig. 6) exhibited an extremely unstable trend near the stall. An inspection of the correlation curve in reference 5 indicates that this might be expected because of the combination of aspect ratio and sweep angle incorporated on the model. Other investigations have been concerned with the relief of this unstable trend through the use of various devices such as nose flaps and slots and stall-control vanes. It was felt, however, that the unstable moment curve would not appreciably affect the principal results obtained through the use of negative dihedral, tip droop, or the various tip-shape modifications.

Effect of negative geometric dihedral.- The use of -10° geometric dihedral in the wing had no beneficial effect on the unstable variation of the pitching-moment curve near the stall or on the slope $C_{m_{C_L}}$ in the low-lift range (figs. 6 and 7(a)).

Effect of tip droop.- No beneficial effect on the pitching-moment characteristics at the stall occurred as a result of drooping the wing tips 45°.

The drooped tips had no effect on $C_{m_{C_L}}$ but did produce a change in the pitching moment at zero lift (figs. 6 and 8(a)) since the tips were deflected at an angle to the relative wind in a manner that effectively produced camber at the wing tips similar to that which would result from trailing-edge-flap deflection.

Effect of tip shape.- The variations in wing-tip shape did not improve the unstable pitching-moment characteristics near the stall.

Some variation in the slope $C_{m_{C_L}}$ appeared for the wings with different tips (fig. 9) but the differences are a result of the shift in the quarter chord of the mean aerodynamic chord that accompanies tip changes since all the pitching moments were referred to the quarter chord of the mean aerodynamic chord of the wing with parallel tips (tips 1 and 1a).

Effective Dihedral

Effect of negative geometric dihedral.- An angle of -10° of geometric dihedral was selected since the investigation of reference 1 indicated this to be about the maximum angle feasible. For negative dihedral angles in excess of 10° the angle of attack of the leading wing panel in yaw is so decreased that the trailing wing stalls first, resulting in a rapid increase in effective dihedral.

In the low and moderate lift-coefficient range the use of -10° geometric dihedral in the wing resulted in an average decrease in the effective-dihedral parameter C_{l_ψ} of about 0.0014 from the value for the model with zero dihedral for both the tail-on and tail-off conditions. (See fig. 18.) This corresponds to a value of $C_{l_{\psi_\Gamma}}$ of about 0.00014 as compared to 0.00021 commonly obtained for unswept wings (reference 6), or the swept-wing value obtained was about 65 percent of the unswept-wing value. An investigation of a 40° sweptback wing (reference 1) indicated an average value of $C_{l_{\psi_\Gamma}}$ of 0.00016 or about 75 percent of the unswept-wing value.

For the model with tail on there was little difference between the maximum value of C_{l_ψ} for the basic model and the model with -10° geometric dihedral although the maximum value occurred at a lower lift coefficient for the basic model.

Effect of tip droop.- For the model with the tail unit removed, drooping the wing tips 45° resulted in a 35-percent decrease in the slope $C_{l_{\psi C_L}}$ as well as an average decrease in C_{l_ψ} equivalent to about -14° geometric dihedral. (See figs. 19 and 20.) With the tail on the drooped tips reduced C_{l_ψ} about the same amount at $C_L = 0$ as for the tail-off condition but did not reduce the slope $C_{l_{\psi C_L}}$ and only a slight reduction in maximum C_{l_ψ} was obtained (fig. 19). The cause of this behavior is believed to be associated with a change in the contribution of the vertical tail to C_{l_ψ} resulting from sidewash changes at the vertical tail induced by the altered tip vortex pattern.

Effect of tip shape.- The parallel tip was tested both with a square-cut tip (tip 1a) and a faired tip of revolution (tip 1). (See fig. 5.) The faired tip appeared superior to the square-cut tip because of the reduction in the maximum value of C_{l_ψ} equivalent to about -4° geometric dihedral (fig. 21). Consequently, all the other tip shapes tested were faired.

Variations made in the wing-tip shape while maintaining a constant aspect ratio produced slight changes in the slope $C_{l_{\psi_{C_L}}}$ and in the maximum value of C_{l_ψ} (fig. 21). All of the skewed tips (2, 3, and 4) produced larger rolling moments with yaw than either the parallel or circular tip (1 and 5). The maximum decrease in $C_{l_{\psi_{C_L}}}$ occurred between tips 3 and 5 and amounted to about a 30-percent reduction. The maximum reduction in C_{l_ψ} occurred between tips 3 and 5 and was equivalent to about -8.5° of geometric dihedral. The circular tip appeared only slightly better than the faired parallel tip.

Directional and Lateral-Force Characteristics

Effect of negative geometric dihedral.- The use of -10° geometric dihedral in the wing resulted in slight increases in the lateral-force parameter C_{Y_ψ} and slightly increased the directional stability C_{n_ψ} (figs. 13 and 14(a)). Similar results were shown in reference 1.

Effect of tip droop.- Drooping the wing tips 45° caused a slight increase in C_{Y_ψ} but the directional stability C_{n_ψ} was decreased (figs. 13 and 15(a)). It is apparent that the forces on the receding tip in yaw are great enough to cause a tendency toward increasing the yaw angle.

Effect of tip shape.- Changes in the wing-tip shape resulted in slight and inconsistent variations in C_{Y_ψ} and C_{n_ψ} (figs. 13 and 16).

Aileron Effectivenss of Drooped Tip

Deflecting the tip appeared to be an adequate means of maintaining lateral control. In the low-lift range the rolling effectiveness resulting from the right-tip deflection $C_{l_{\delta_{T_R}}}$ was about 0.0008 (figs. 11 and 12). This value of $C_{l_{\delta_{T_R}}}$ is low relative to that considered desirable for airplanes having unswept wings but is about equal to that obtained from tests of similar swept-wing models equipped with conventional

trailing-edge ailerons (reference 7). The rolling effectiveness decreased in the higher lift range to a value about 70 percent of the value in the low-lift range.

The yawing moment accompanying the tip deflection appeared to be no more severe than that observed on similar models having conventional ailerons for deflections up to 20°.

In the landing condition, however, if both tips are given an initial downward deflection for the purpose of reducing C_{l_ψ} and then deflected differentially as ailerons, the lateral control thus provided might become undesirable since past experience has shown that such controls may cause high adverse yaw.

CONCLUDING REMARKS

The results of low-speed tests made to determine the effects of negative geometric dihedral, tip droop, and tip shape on the aerodynamic characteristics of a complete model having a 45° sweptback wing are summarized as follows:

1. The use of -10° geometric dihedral resulted in a reduction in the average value of the effective-dihedral parameter C_{l_ψ} through the low and moderate lift-coefficient range that was about 65 percent as great as that usually obtained for unswept wings.

2. Drooping the wing tips 45° (maintaining the same ground clearance as that with -10° geometric dihedral) resulted in a decrease in the average value of C_{l_ψ} through the low and moderate lift-coefficient range equivalent to about -14° geometric dihedral and also caused an increase in the maximum lift coefficient of 0.15.

3. Changes in the wing-tip plan form indicated that C_{l_ψ} was lowest for the parallel and circular tips and highest for the tips skewed either in or out.

4. By changing a square-cut tip to a faired tip of revolution, the maximum value of C_{l_ψ} for the model with parallel tips was reduced by an amount equivalent to about -4° geometric dihedral.

5. Deflecting the wing tip (from zero) resulted in rolling and yawing moments about the same as that produced by a conventional aileron on a similar sweptback-wing model.

Langley Aeronautical Laboratory
National Advisory Committee for Aeronautics
Langley Field, Va.

REFERENCES

1. Maggin, Bernard, and Shanks, Robert E.: The Effect of Geometric Dihedral on the Aerodynamic Characteristics of a 40° Swept-Back Wing of Aspect Ratio 3. NACA TN No. 1169, 1946.

2. Letko, William, and Goodman, Alex: Preliminary Wind-Tunnel Investigation at Low Speed of Stability and Control Characteristics of Swept-Back Wings. NACA TN No. 1046, 1946.

3. Gillis, Clarence L., Polhamus, Edward C., and Gray, Joseph L., Jr.: Charts for Determining Jet-Boundary Corrections for Complete Models in 7- by 10-Foot Closed Rectangular Wind Tunnels. NACA ARR No. L5G31, 1945.

4. Thom, A.: Blocking Corrections in a Closed High-Speed Tunnel. R. & M. No. 2033, British A.R.C., 1943.

5. Shortal, Joseph A., and Maggin, Bernard: Effect of Sweepback and Aspect Ratio on Longitudinal Stability Characteristics of Wings at Low Speeds. NACA TN No. 1093, 1946.

6. Shortal, Joseph A.: Effect of Tip Shape and Dihedral on Lateral-Stability Characteristics. NACA Rep. No. 548, 1935.

7. Lockwood, Vernard E., and Watson, James M.: Stability and Control Characteristics at Low Speed of an Airplane Model Having a 38.7° Sweptback Wing with Aspect Ratio 4.51, Taper Ratio 0.54, and Conventional Tail Surfaces. NACA TN No. 1742, 1948.

TABLE I

GEOMETRIC CHARACTERISTICS OF BASIC MODEL

Wing:	
Area, sq ft	8.323
Span, ft	5.870
Aspect ratio	4.14
Sweepback of quarter-chord line, deg	45
Taper ratio	0.412
Incidence, deg	0
M.A.C., ft	1.464
Root chord, ft	2.007
Tip chord, ft	0.828
Airfoil section	NACA 65-110
Horizontal tail:	
Area, sq ft	1.625
Span, ft	2.85
Aspect ratio	5
Airfoil section	NACA 65-008
Vertical tail:	
Area (not including dorsal), sq ft	1.600
Airfoil section	NACA 65-008

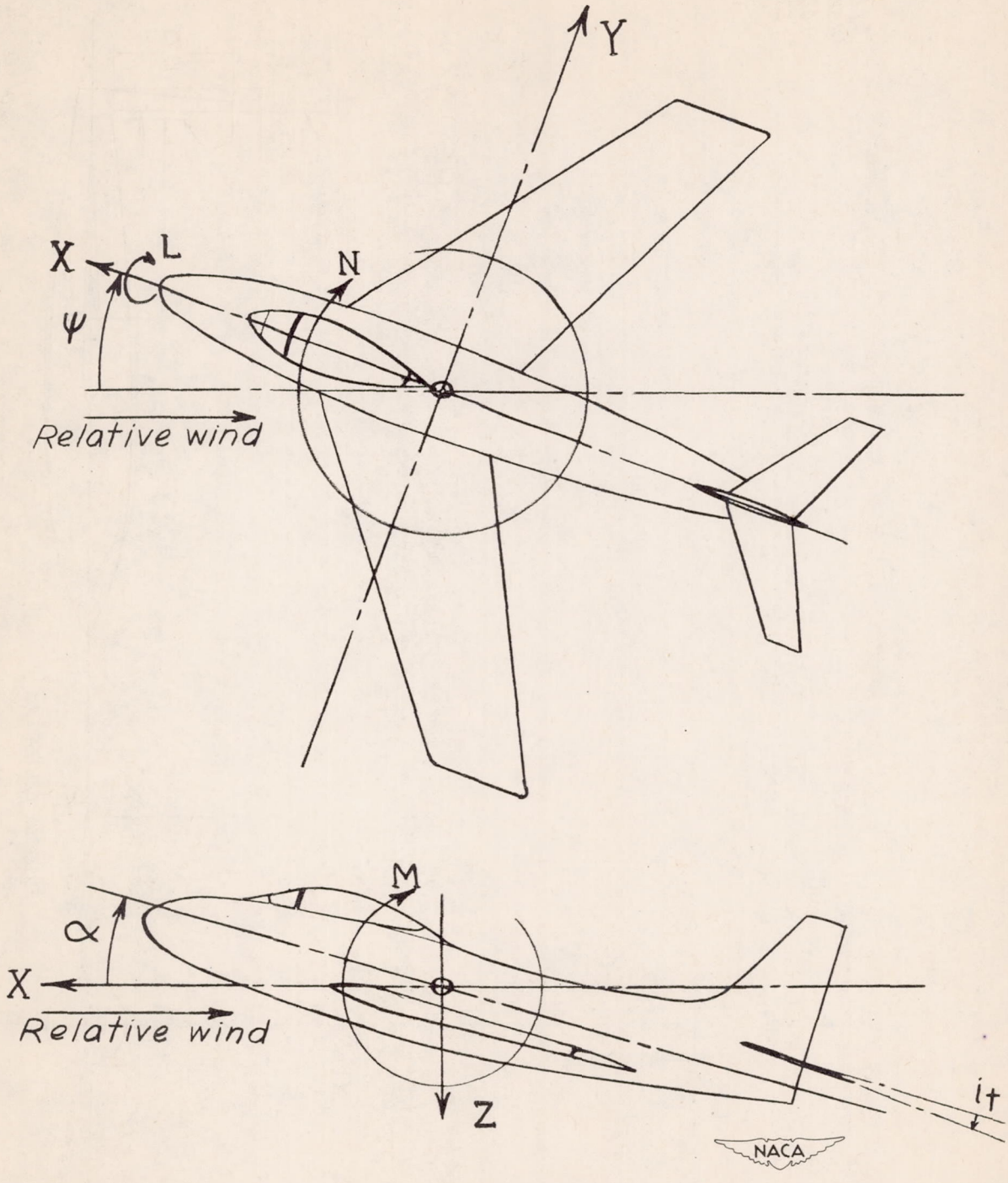

Figure 1.- System of stability axes. Positive forces, moments, and angles indicated by arrows.

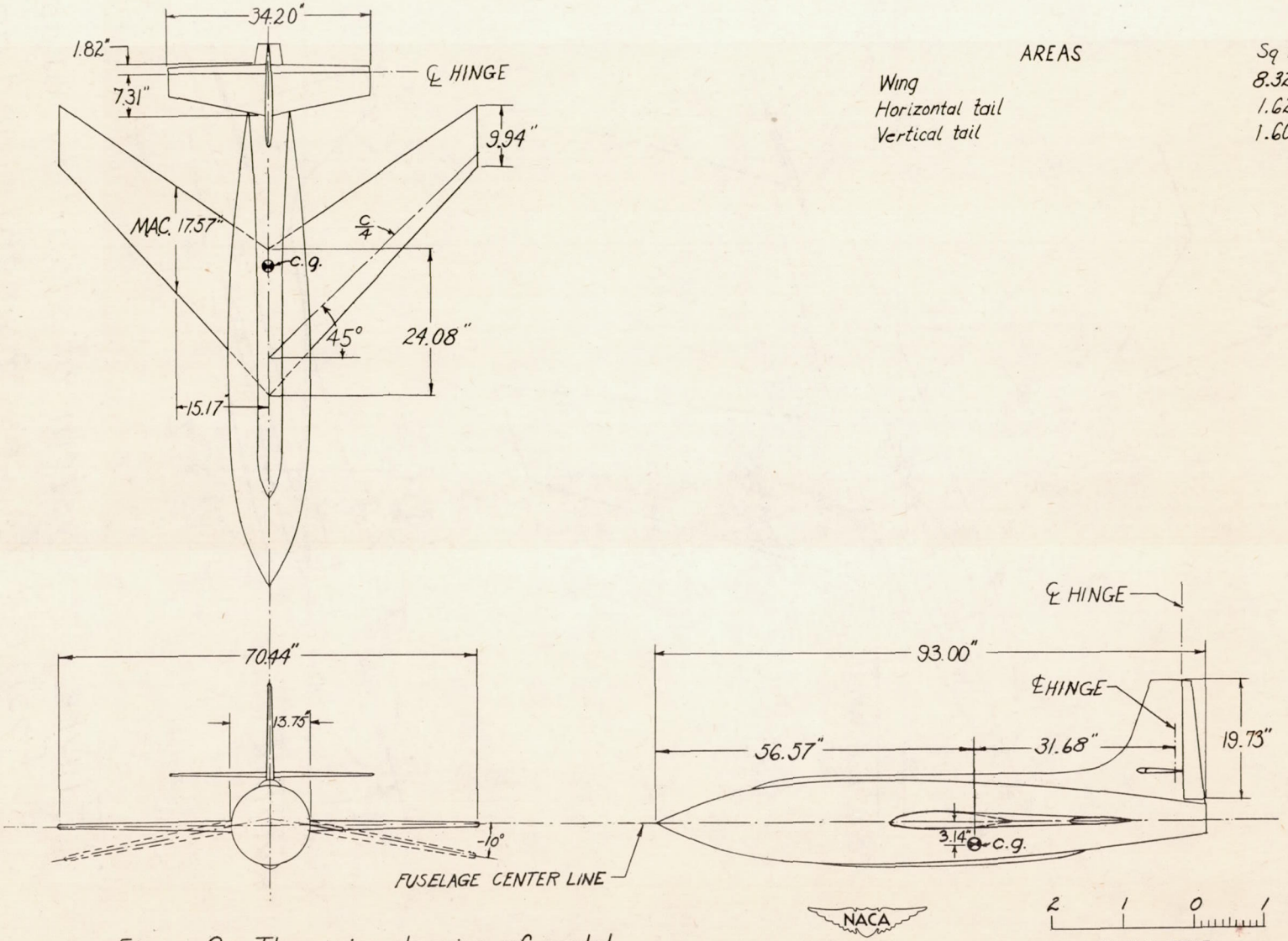

AREAS	Sq ft
Wing	8.323
Horizontal tail	1.625
Vertical tail	1.600

Figure 2.- Three-view drawing of model.

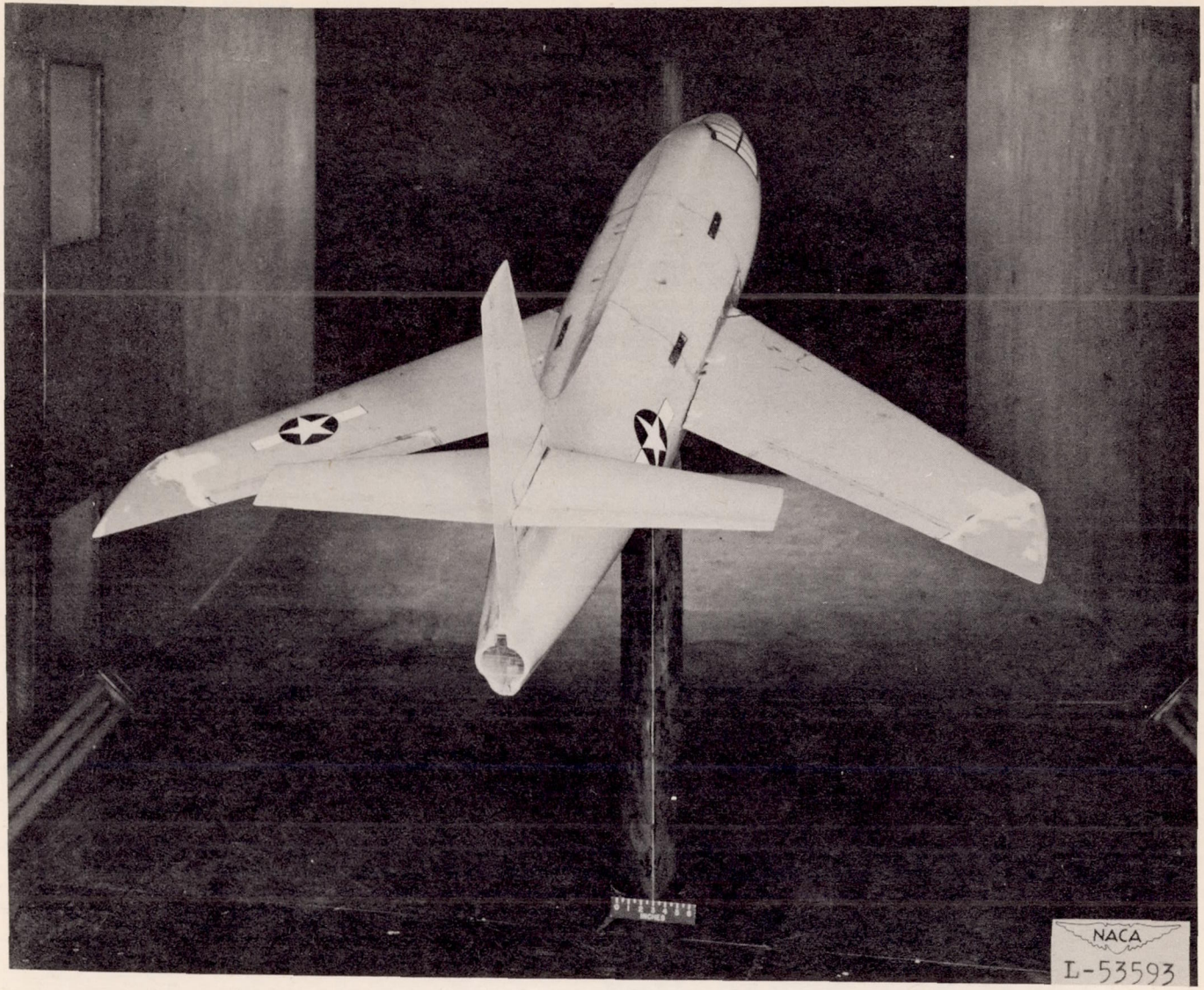

Figure 3.- Basic model mounted in Langley 300 MPH 7- by 10-foot tunnel.

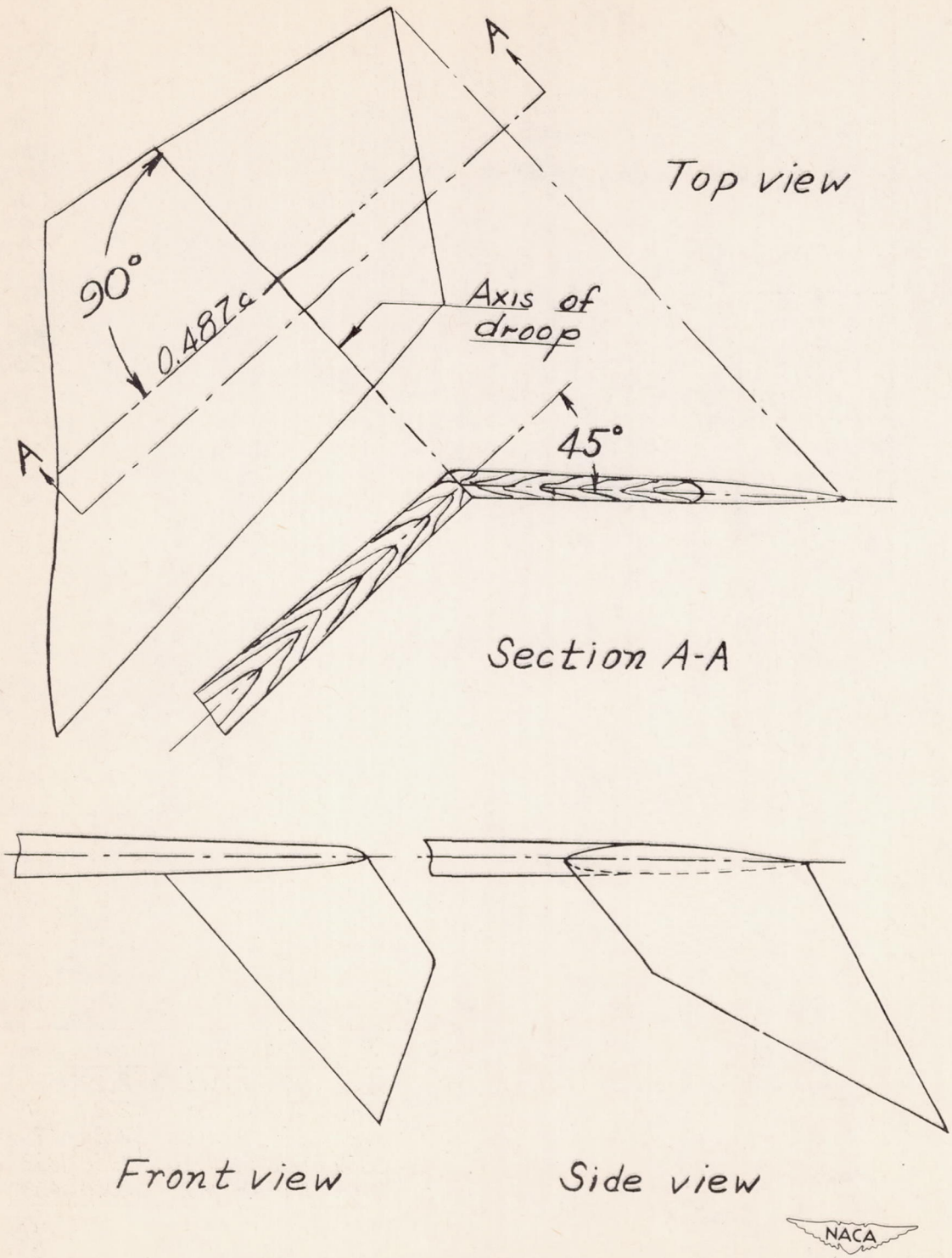

Figure 4.- Details of drooped wing tip.

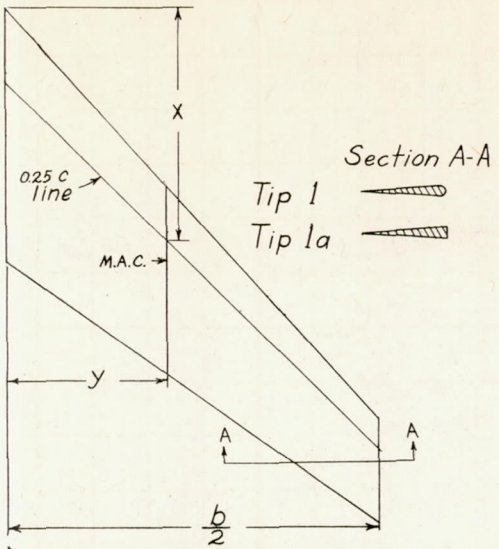

Section A-A

Tip 1

Tip 1a

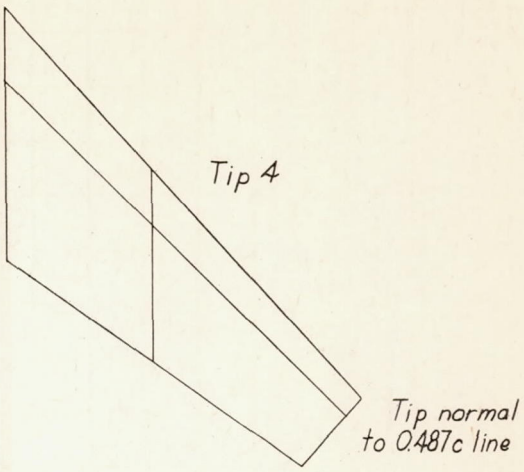

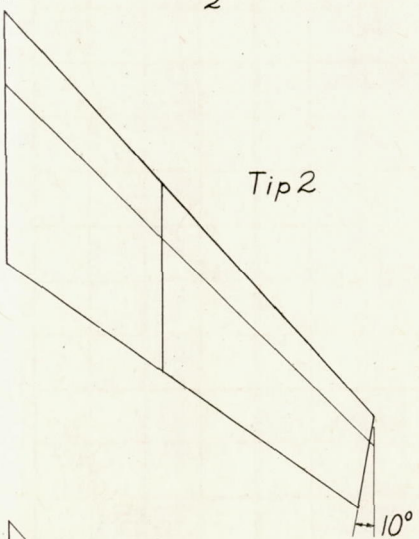

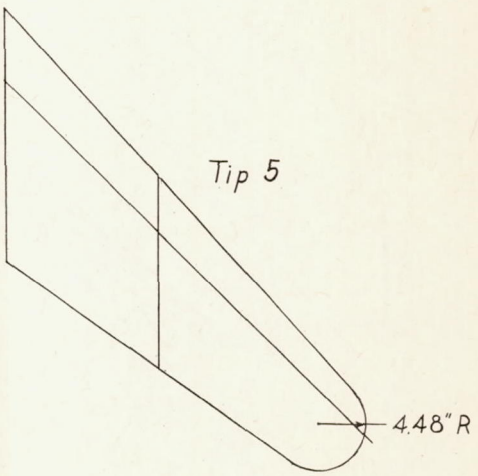

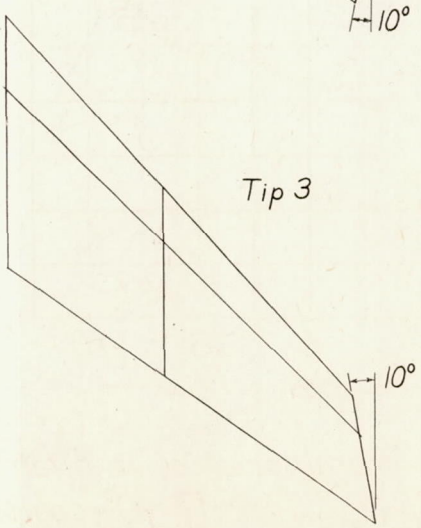

Tip	b/2, in.	S, sq in.	M.A.C., in.	x, in.	y, in.	A
1	35.22	1198.44	17.57	21.24	15.17	4.14
2	34.81	1174.42	18.09	20.93	14.77	4.13
3	34.81	1167.88	18.05	20.85	14.71	4.15
4	33.60	1102.32	18.50	19.86	13.72	4.10
5	34.06	1141.78	18.25	20.53	14.38	4.06

NACA

Figure 5.- Details of wing plan forms with various tips.

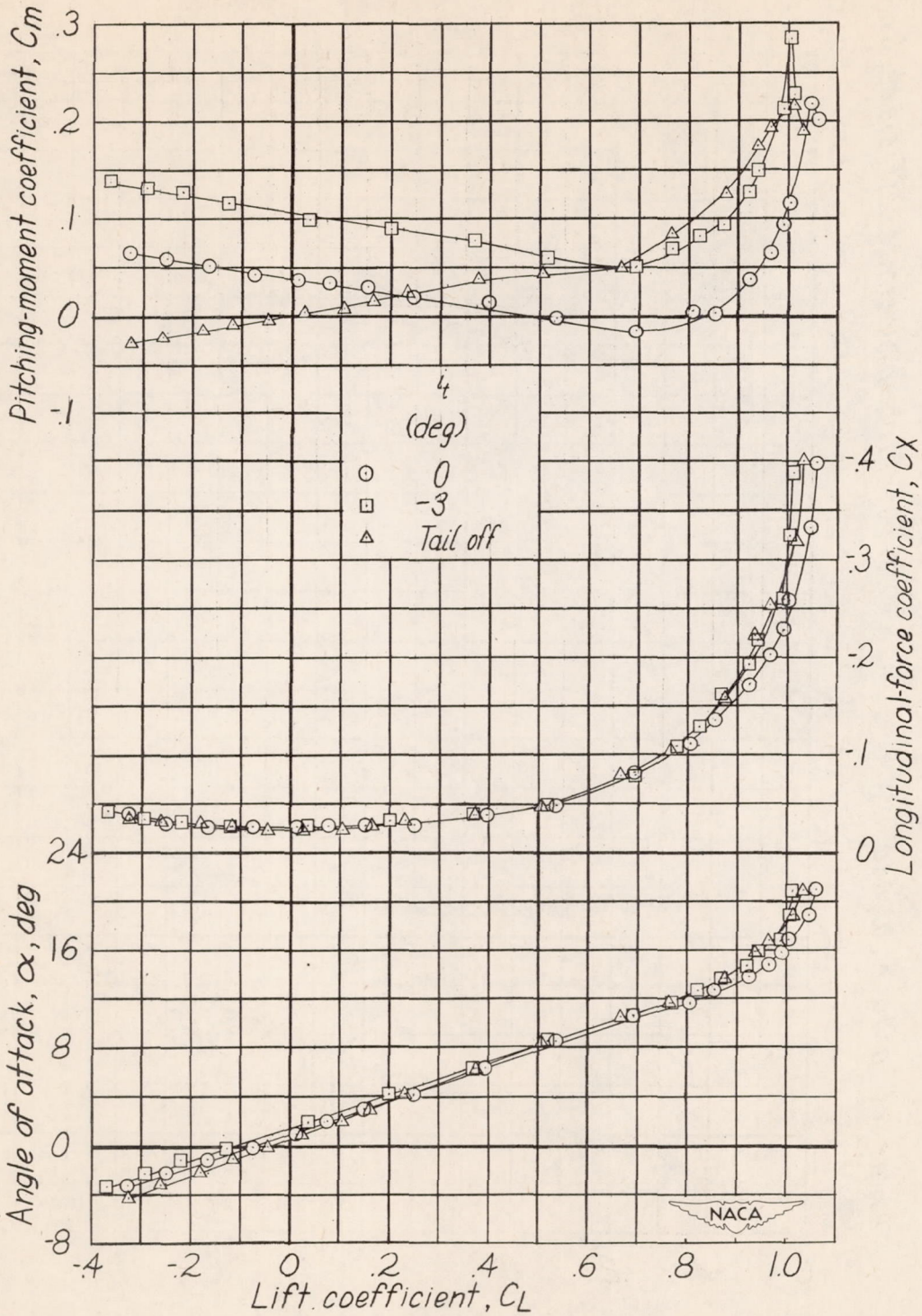

Figure 6.- The aerodynamic characteristics in pitch for the basic model. Tip 1; Γ_W and $\Gamma_T = 0°$; complete model.

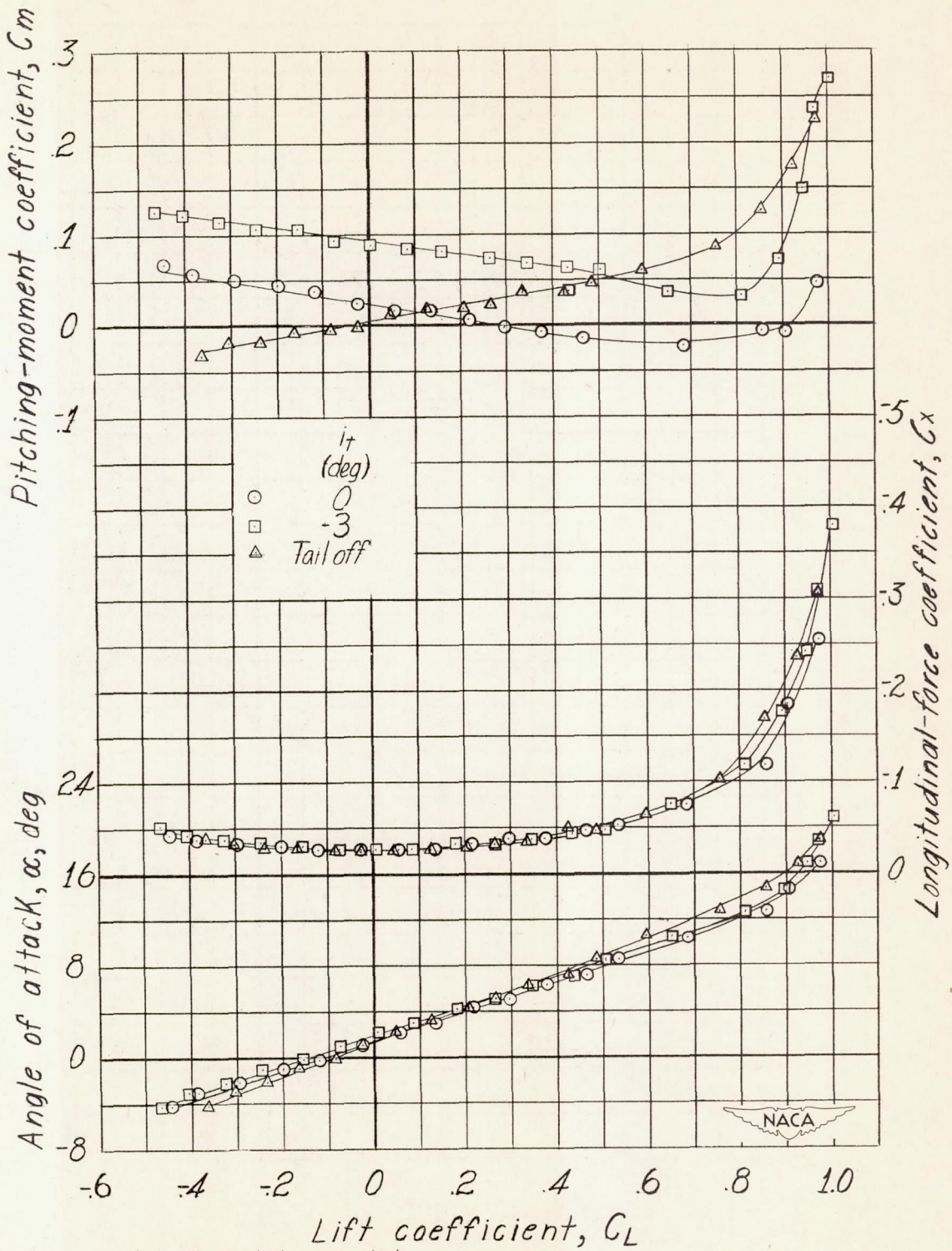

(a) Complete model.

Figure 7.- The aerodynamic characteristics in pitch.

$\Gamma_w = -10°$; tip 1.

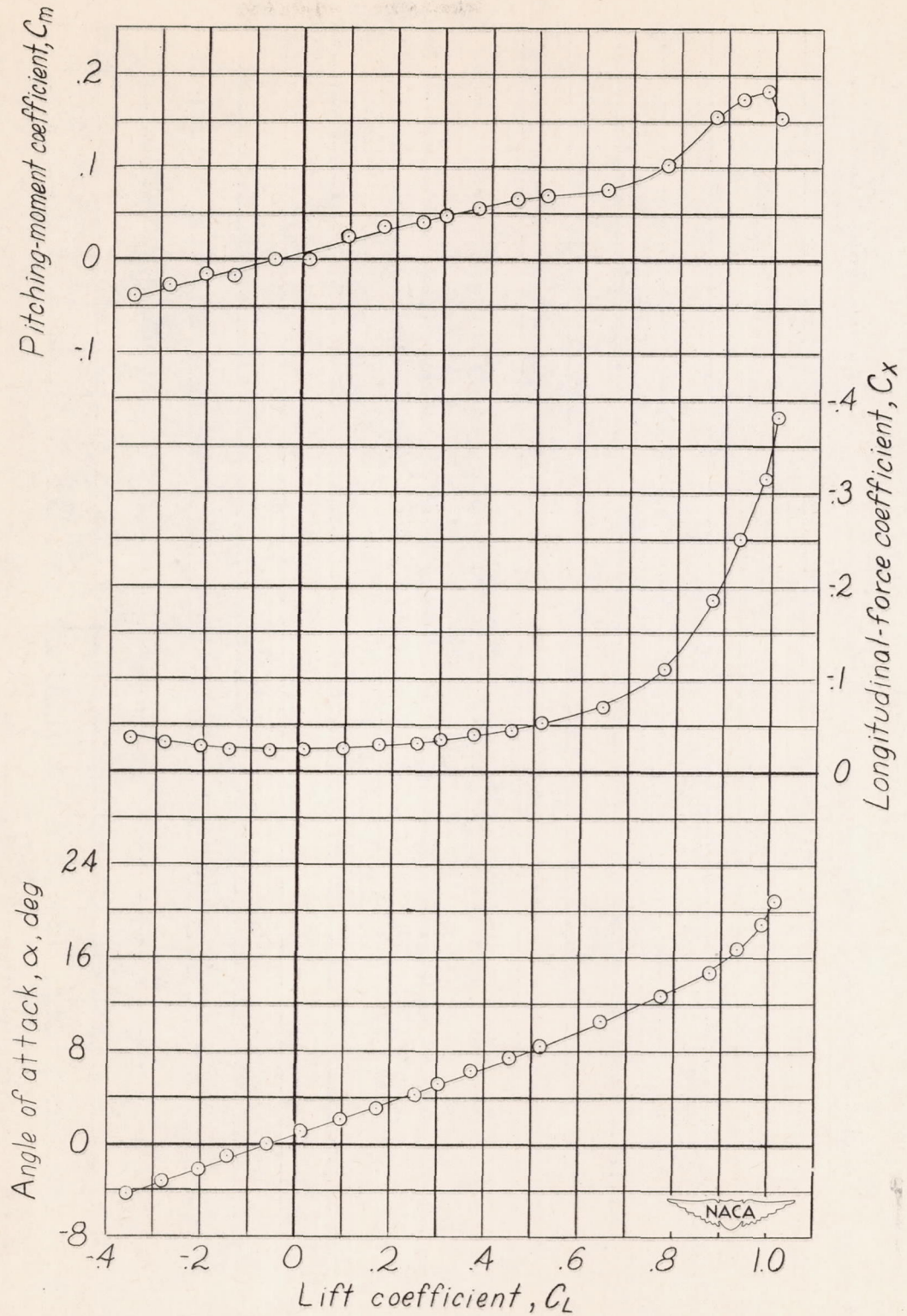

(b) Vertical and horizontal tail off.

Figure 7.- Concluded.

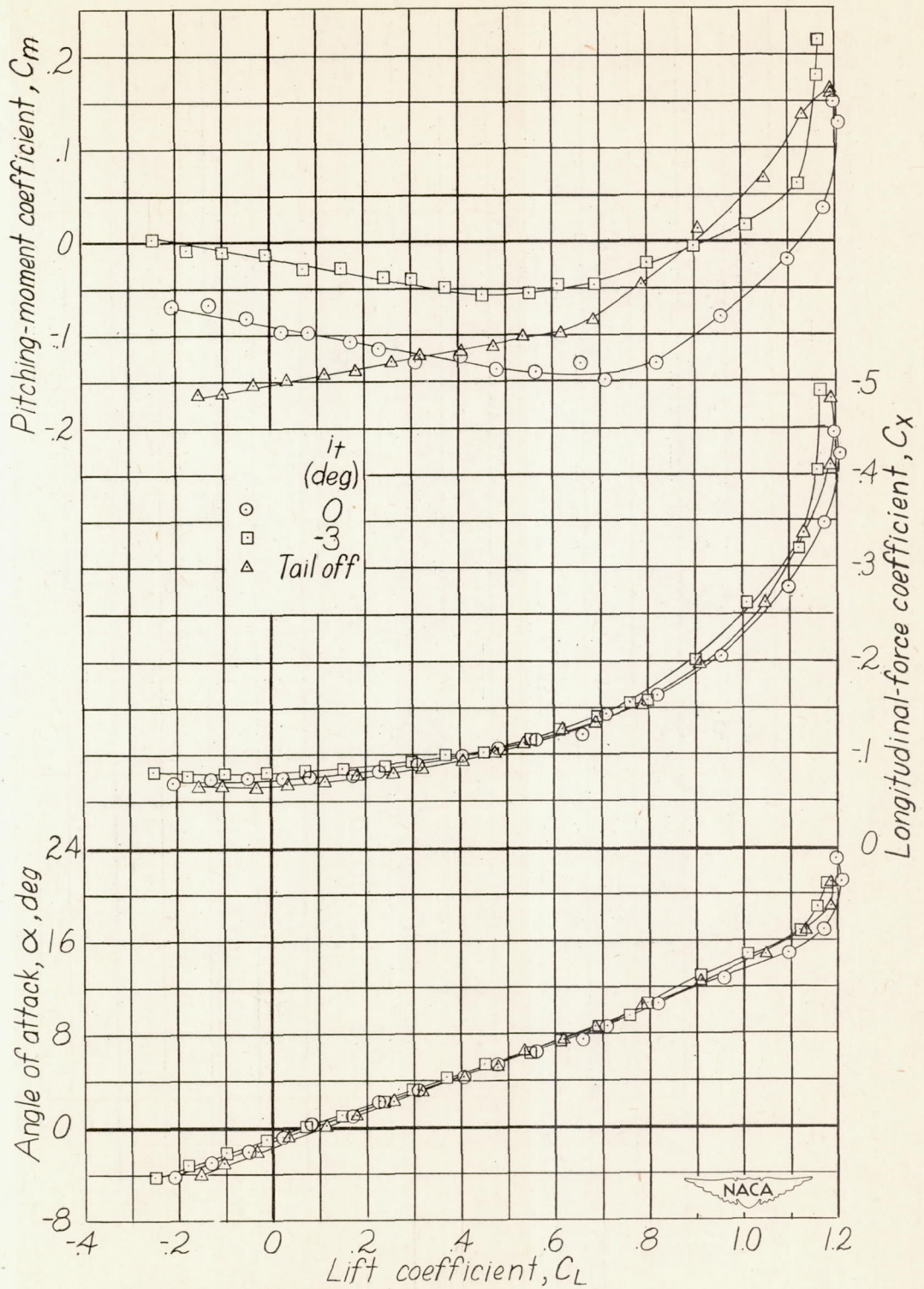

(a) Complete model.

Figure 8.- The aerodynamic characteristics in pitch. $\Gamma_T = -45°$; tip 1.

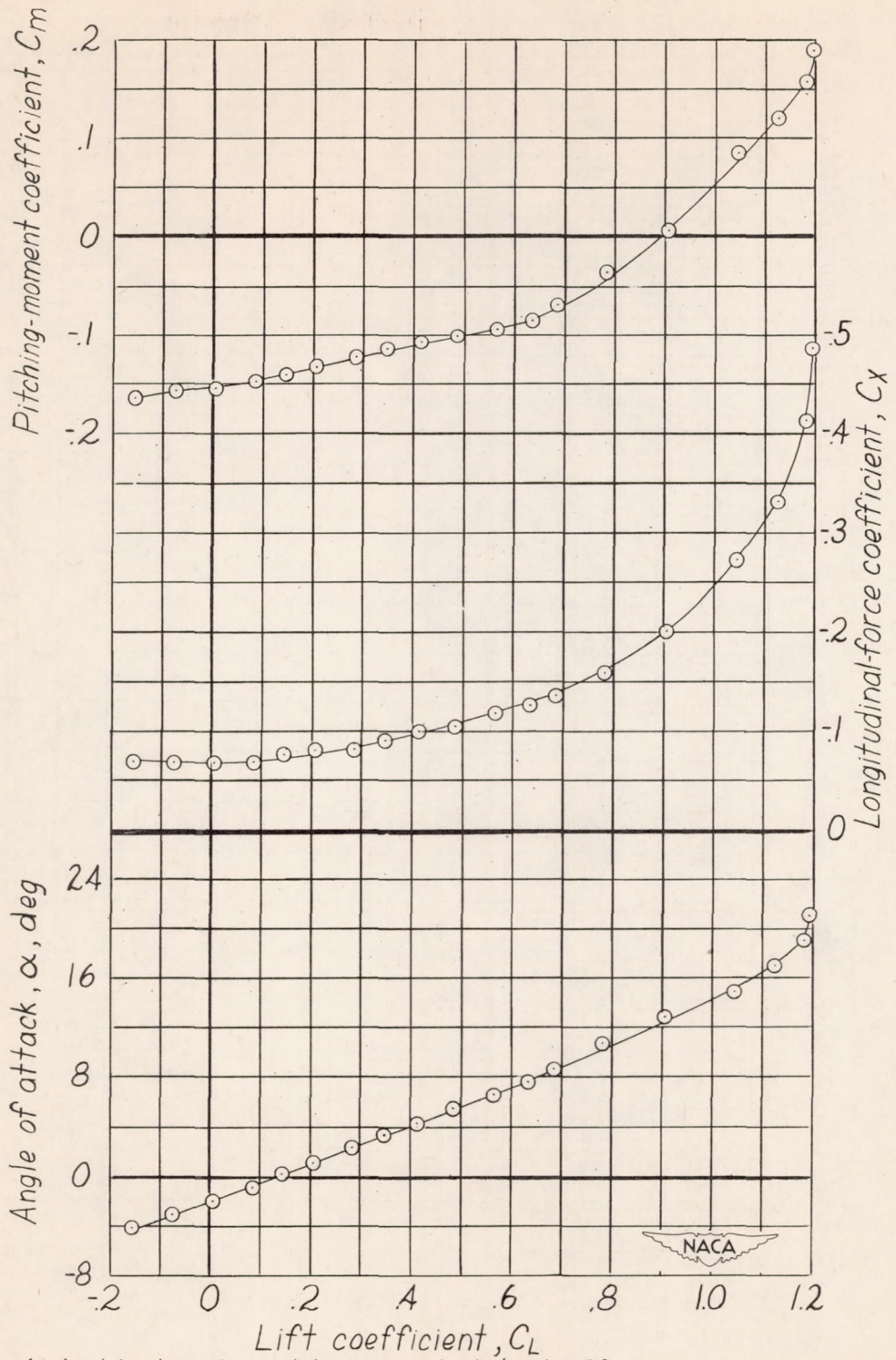

(b) Vertical and horizontal tail off.

Figure 8.- Concluded.

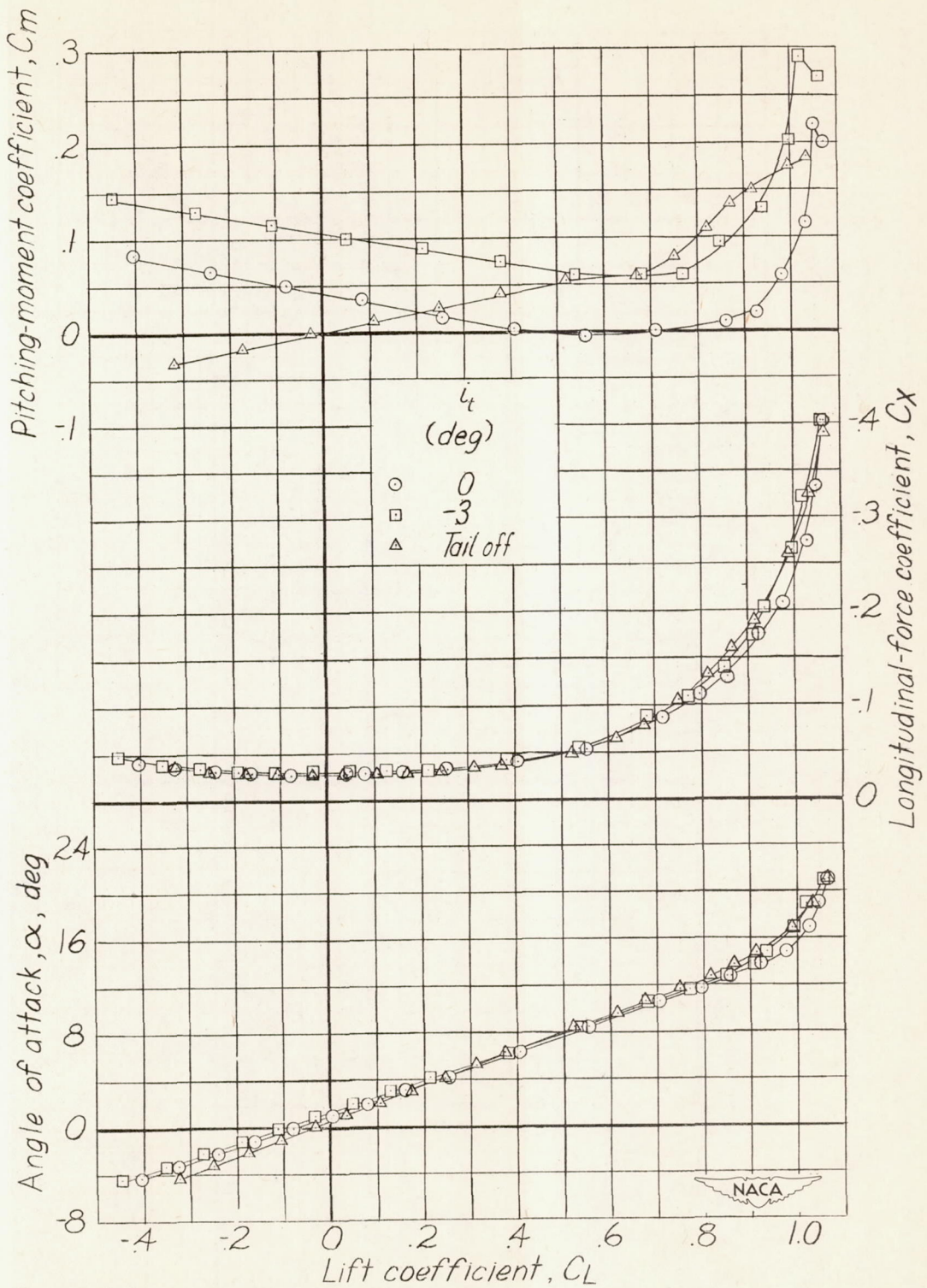

(a) Tip 1a.

Figure 9.- The aerodynamic characteristics in pitch for various tip modifications. Complete model.

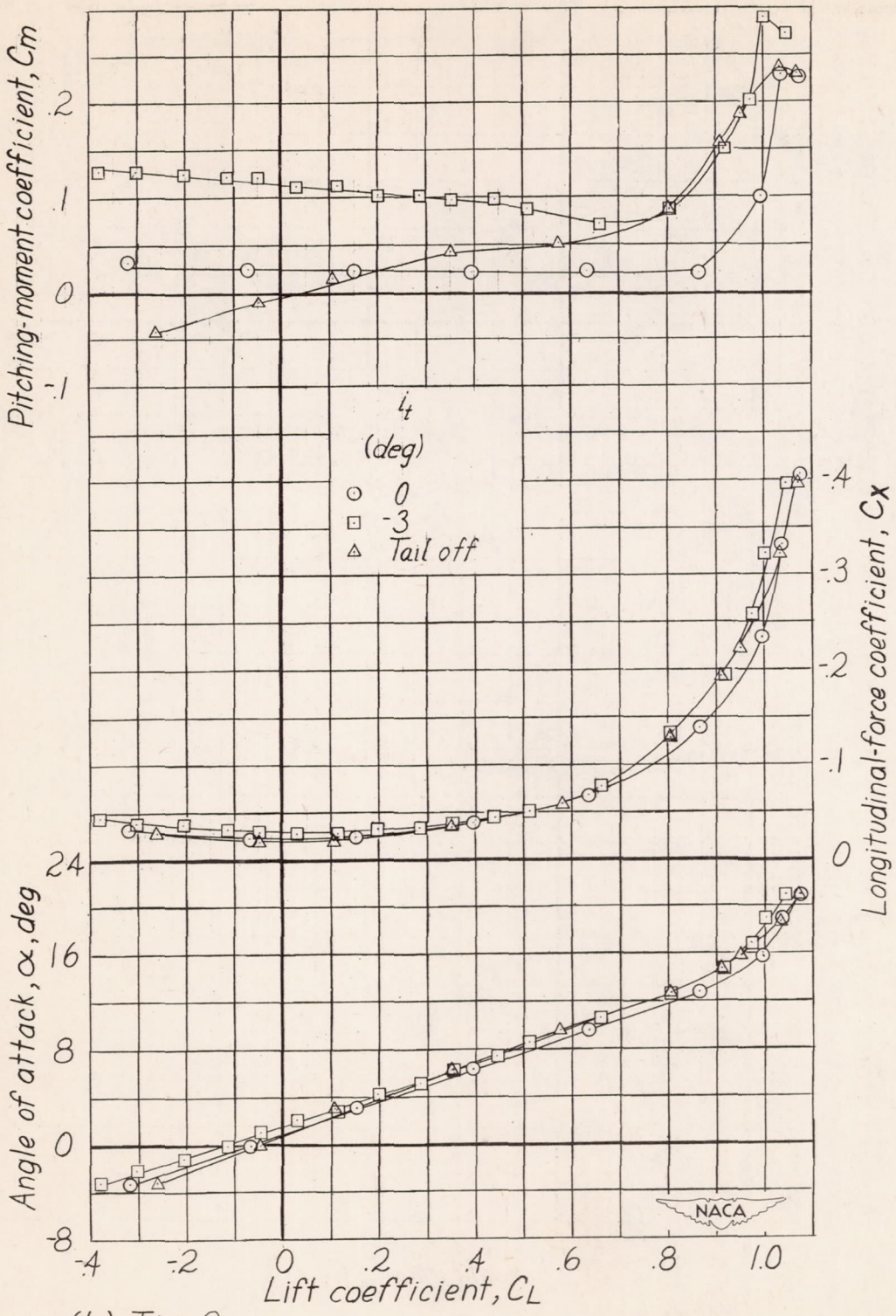

(b) Tip 2.

Figure 9.- Continued.

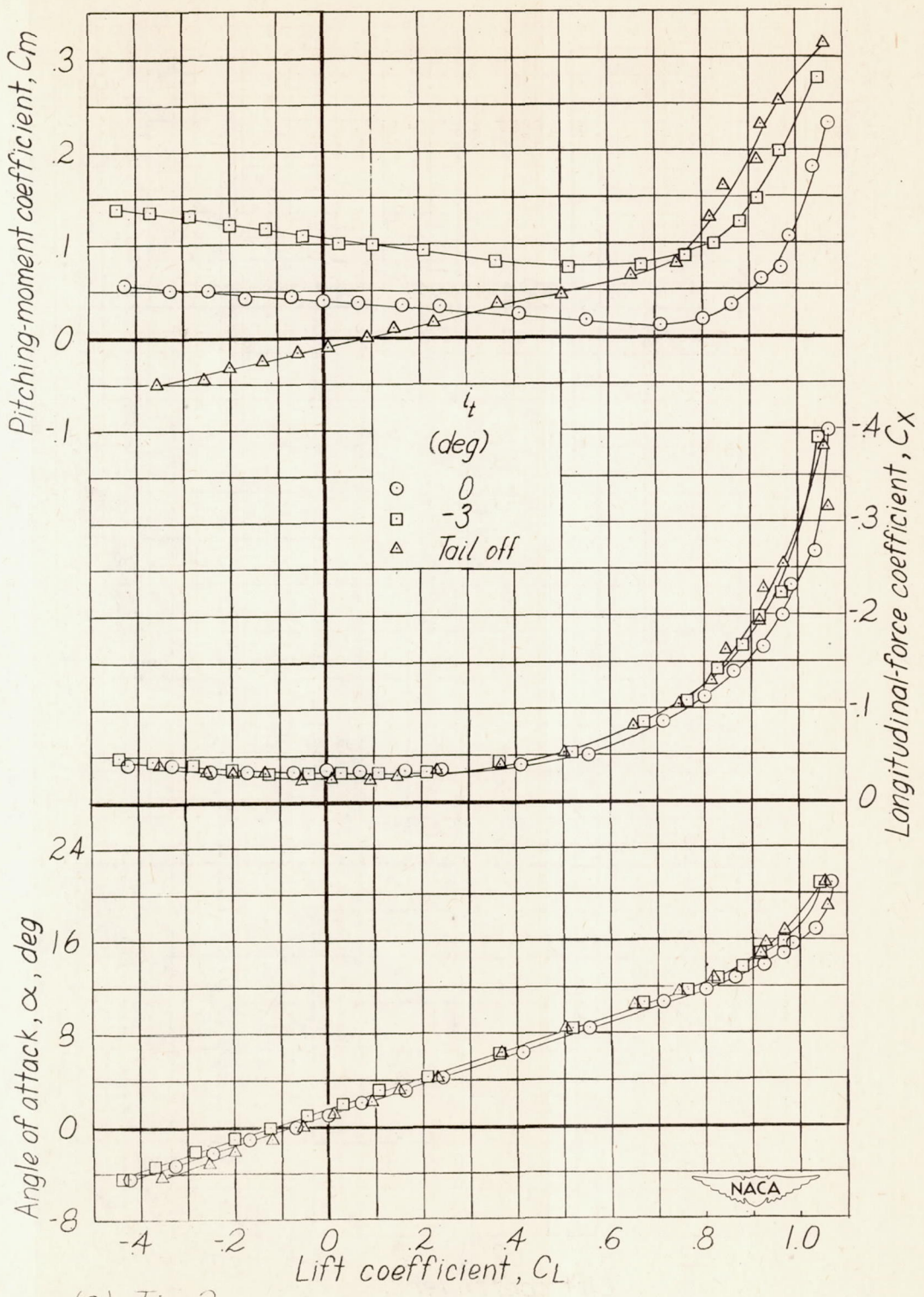

(c) Tip 3

Figure 9.- Continued.

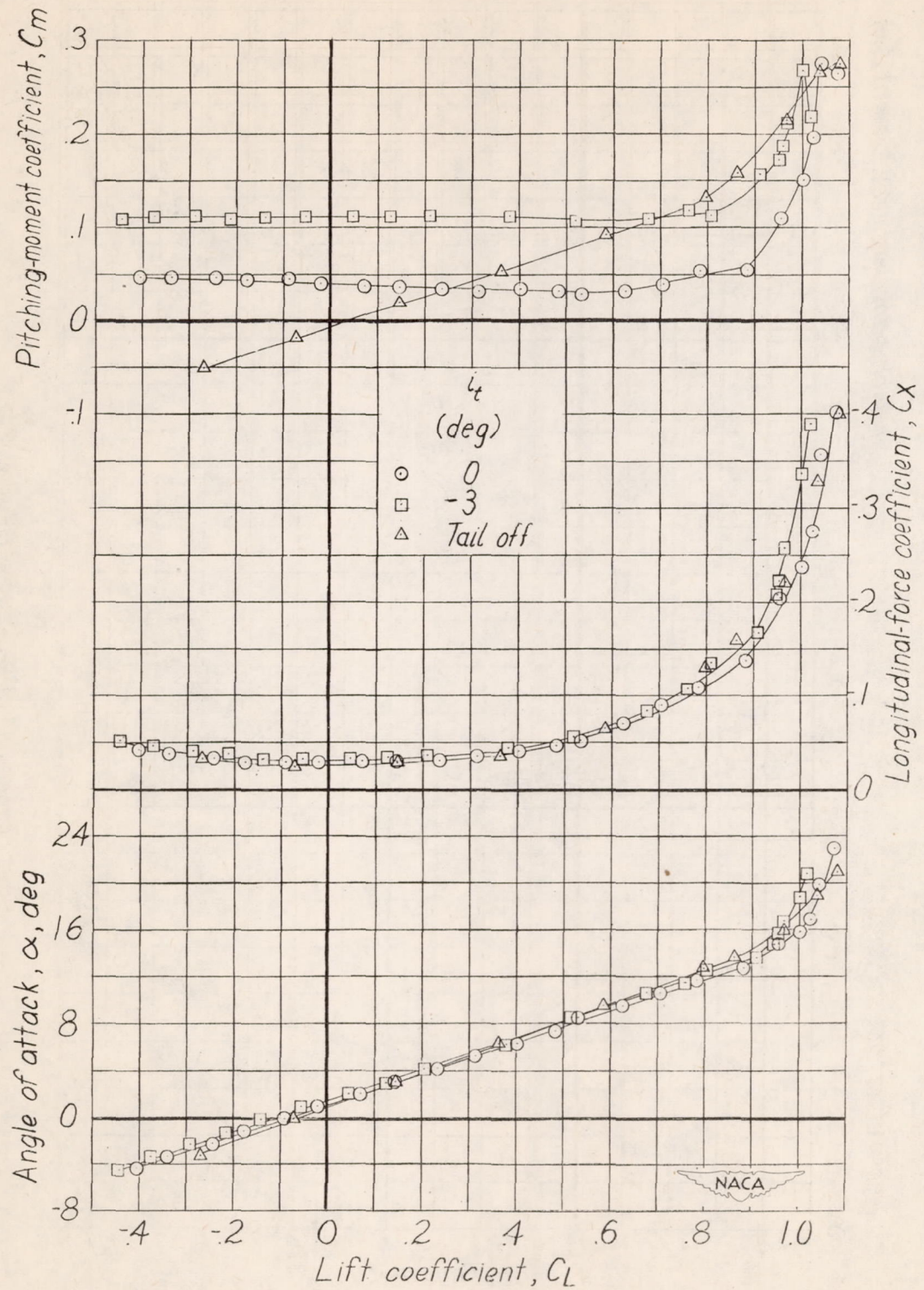

(d) Tip 4

Figure 9.- Continued

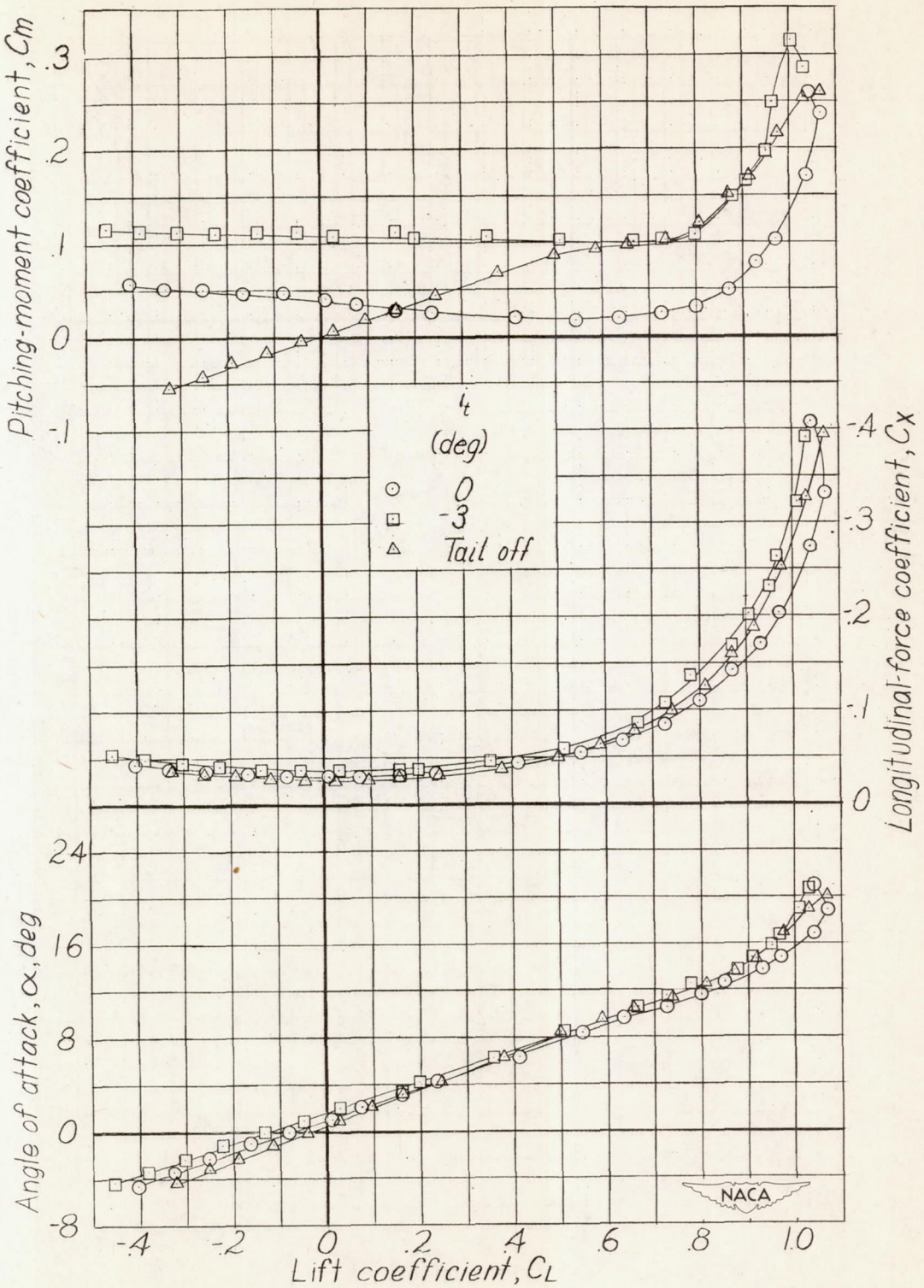

(e) Tip 5

Figure 9.- Concluded.

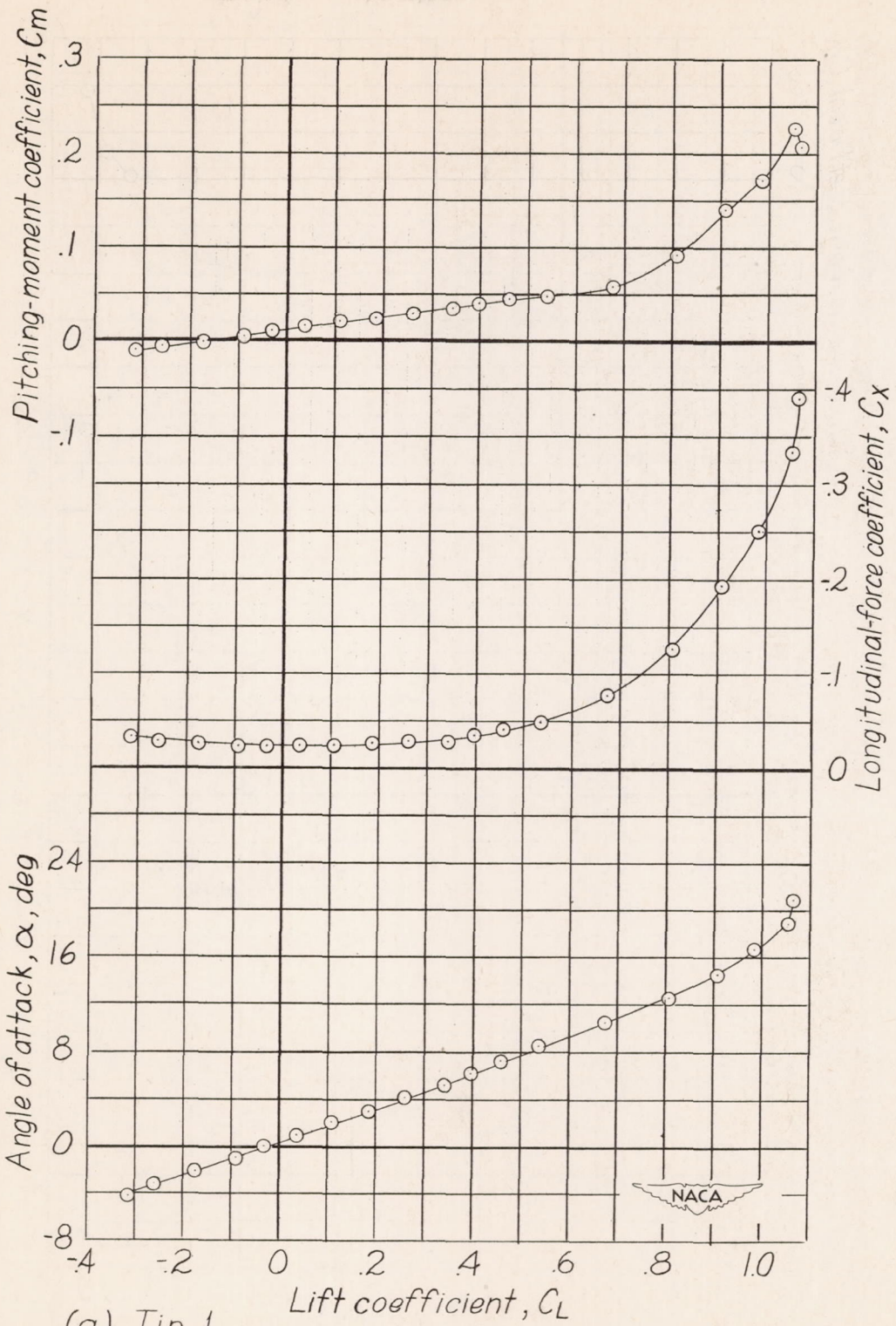

(a) Tip 1.

Figure 10.- The aerodynamic characteristics in pitch for various tip modifications. Vertical and horizontal tail off.

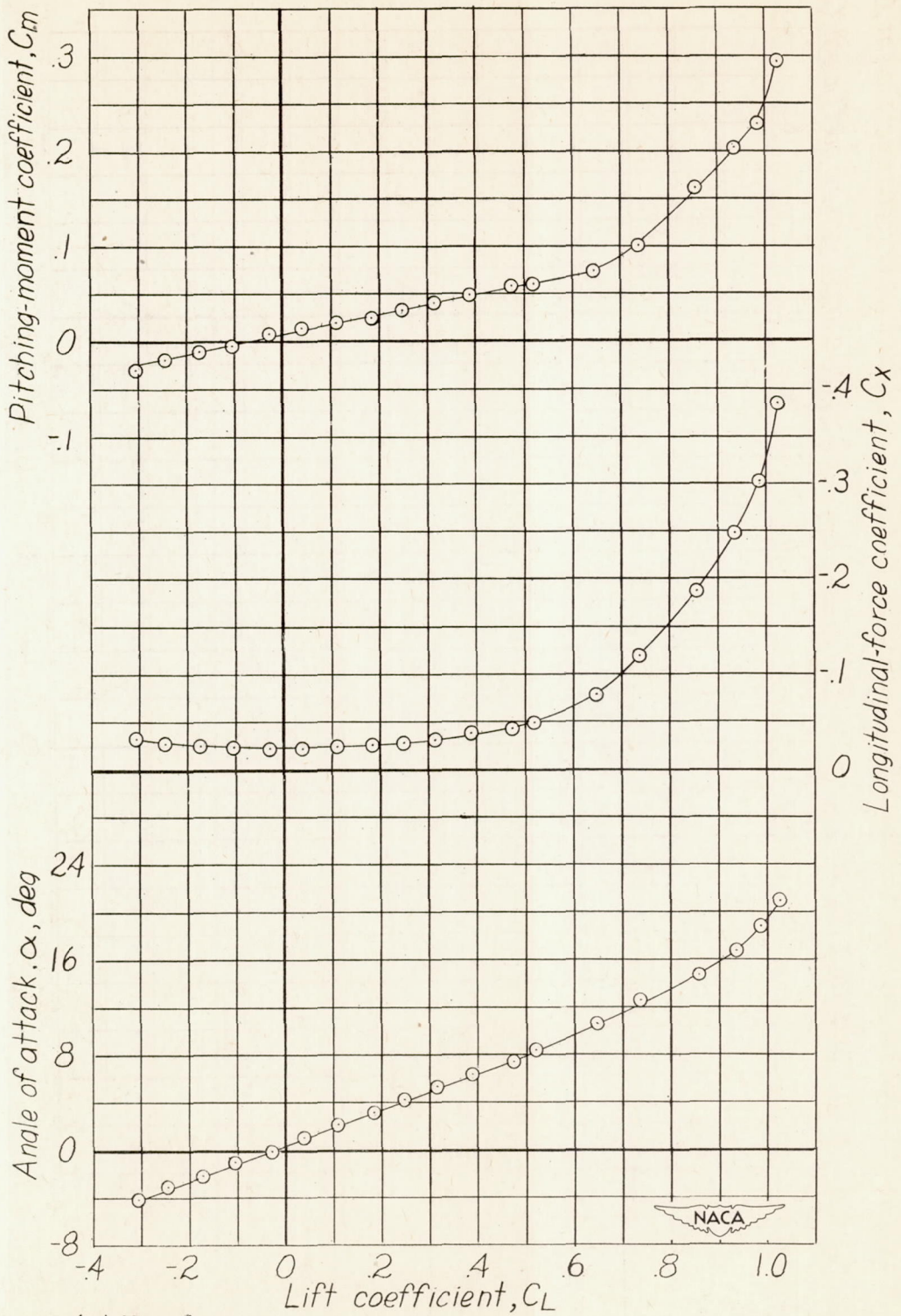

(b) Tip 3

Figure 10 - Concluded

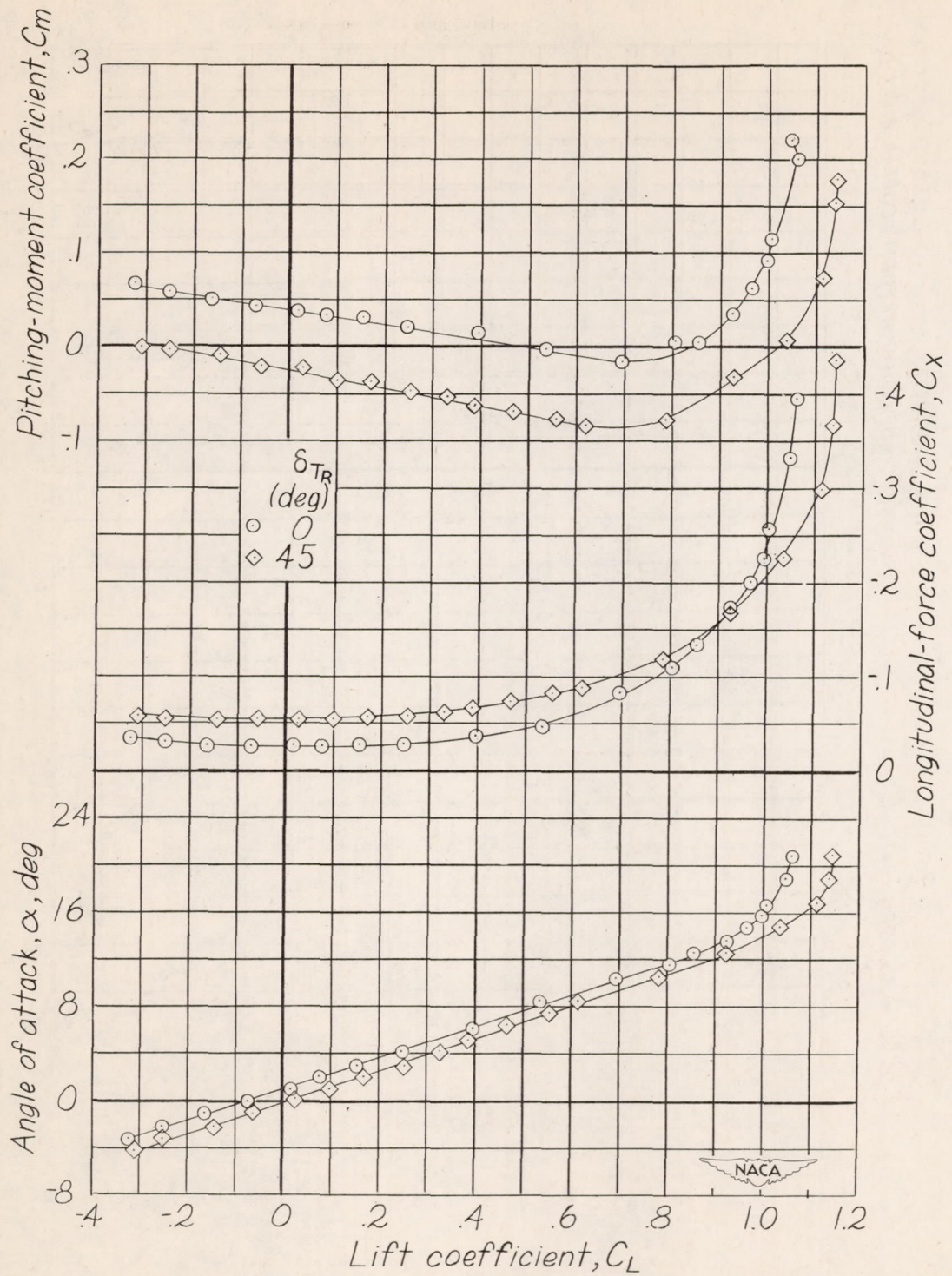

Figure 11.- The effect of right tip deflection on the aerodynamic characteristics in pitch. Complete model. $\delta_{T_L} = 0°$.

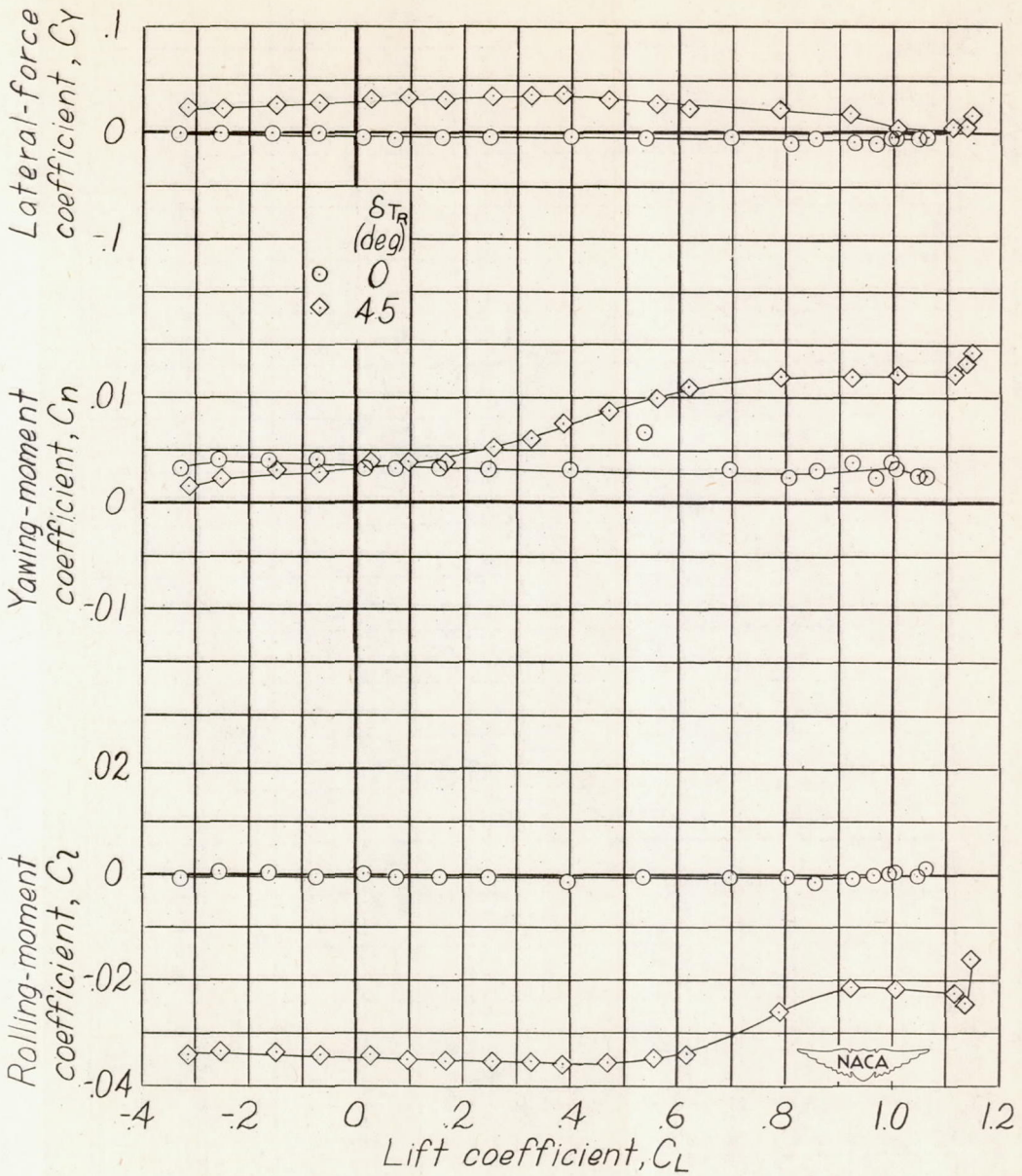

Figure 11.- Concluded.

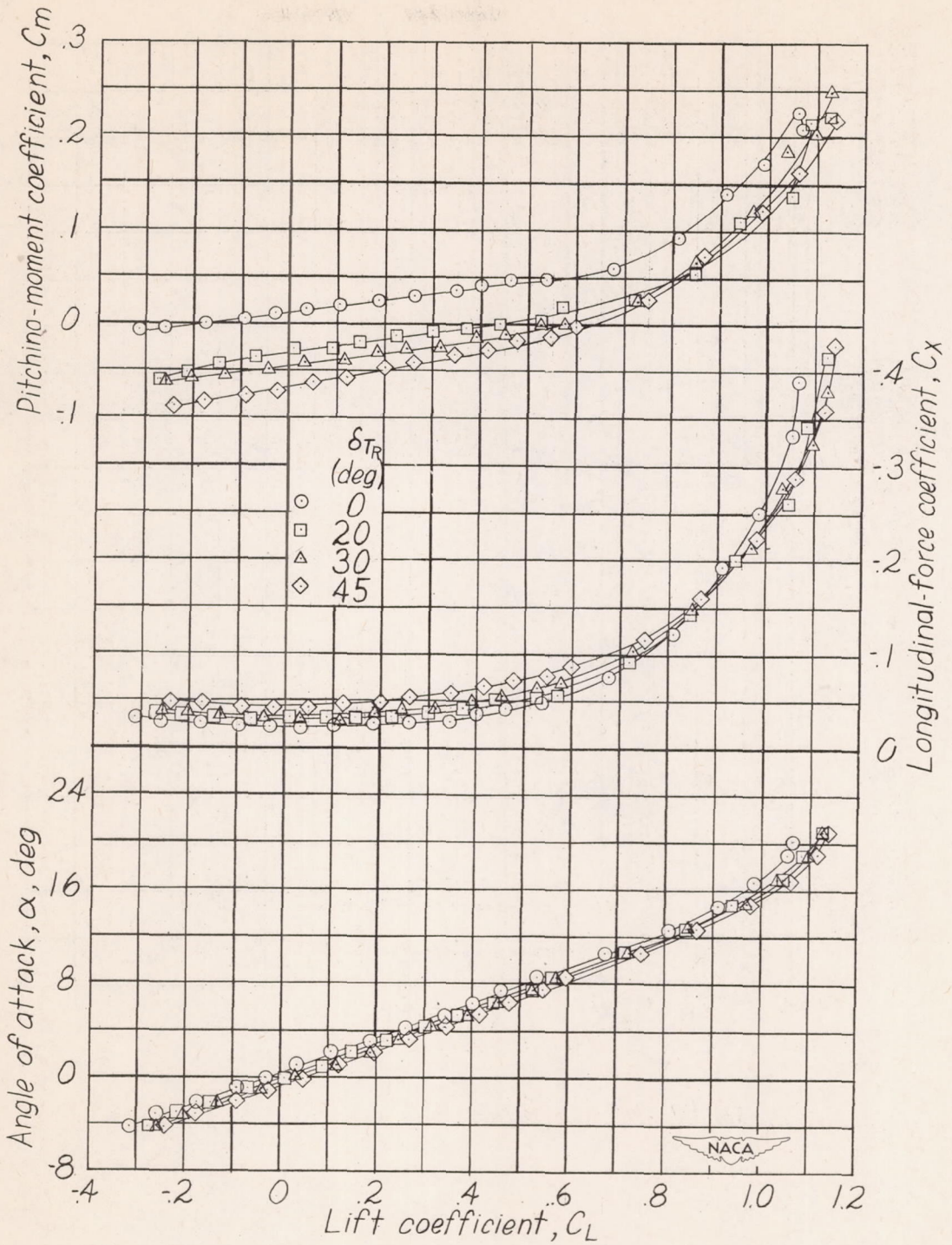

Figure 12.- The effect of right tip deflection on the aerodynamic characteristics in pitch. Vertical and horizontal tail off. $\delta_{T_L} = 0°$.

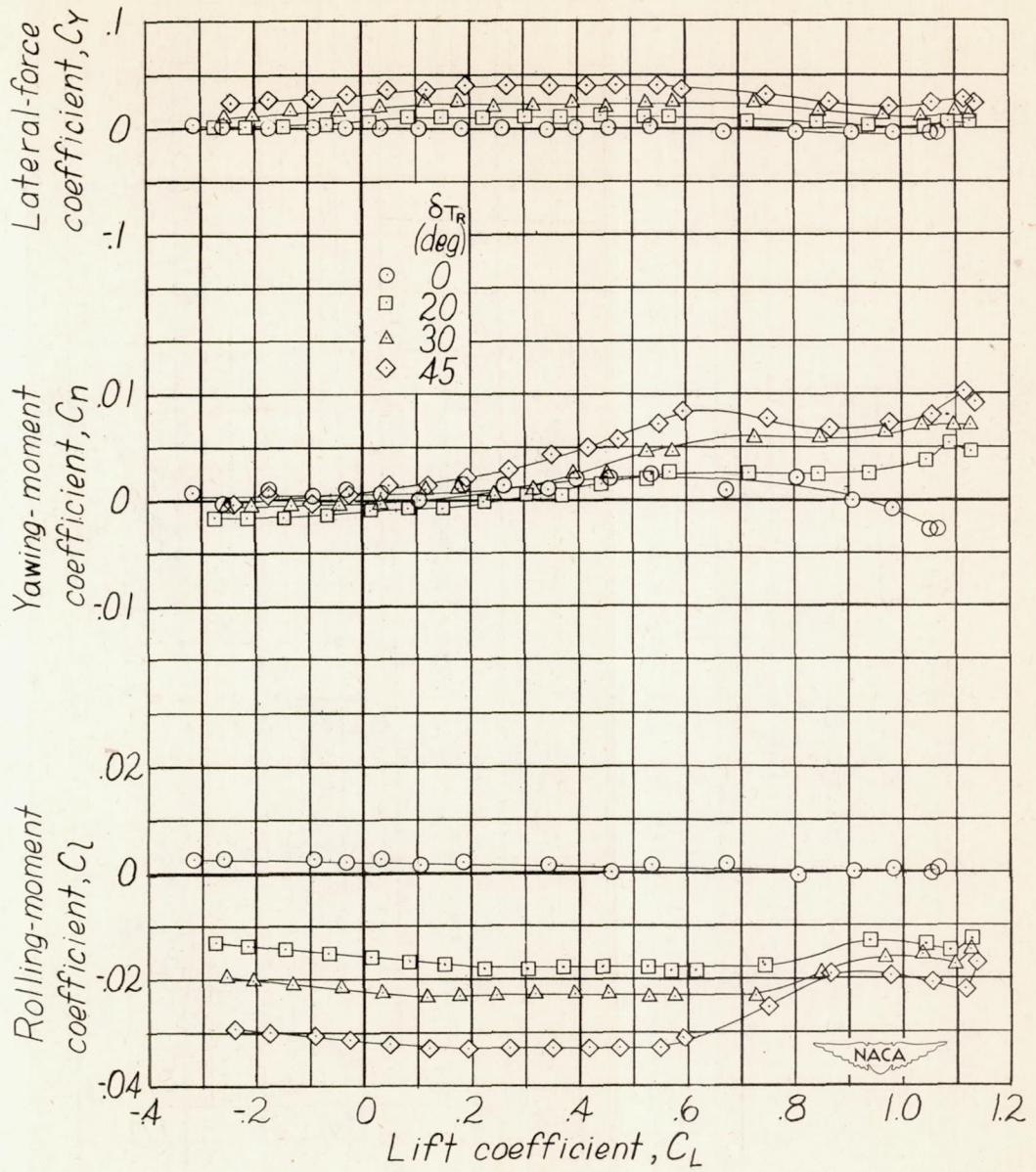

Figure 12.- Concluded.

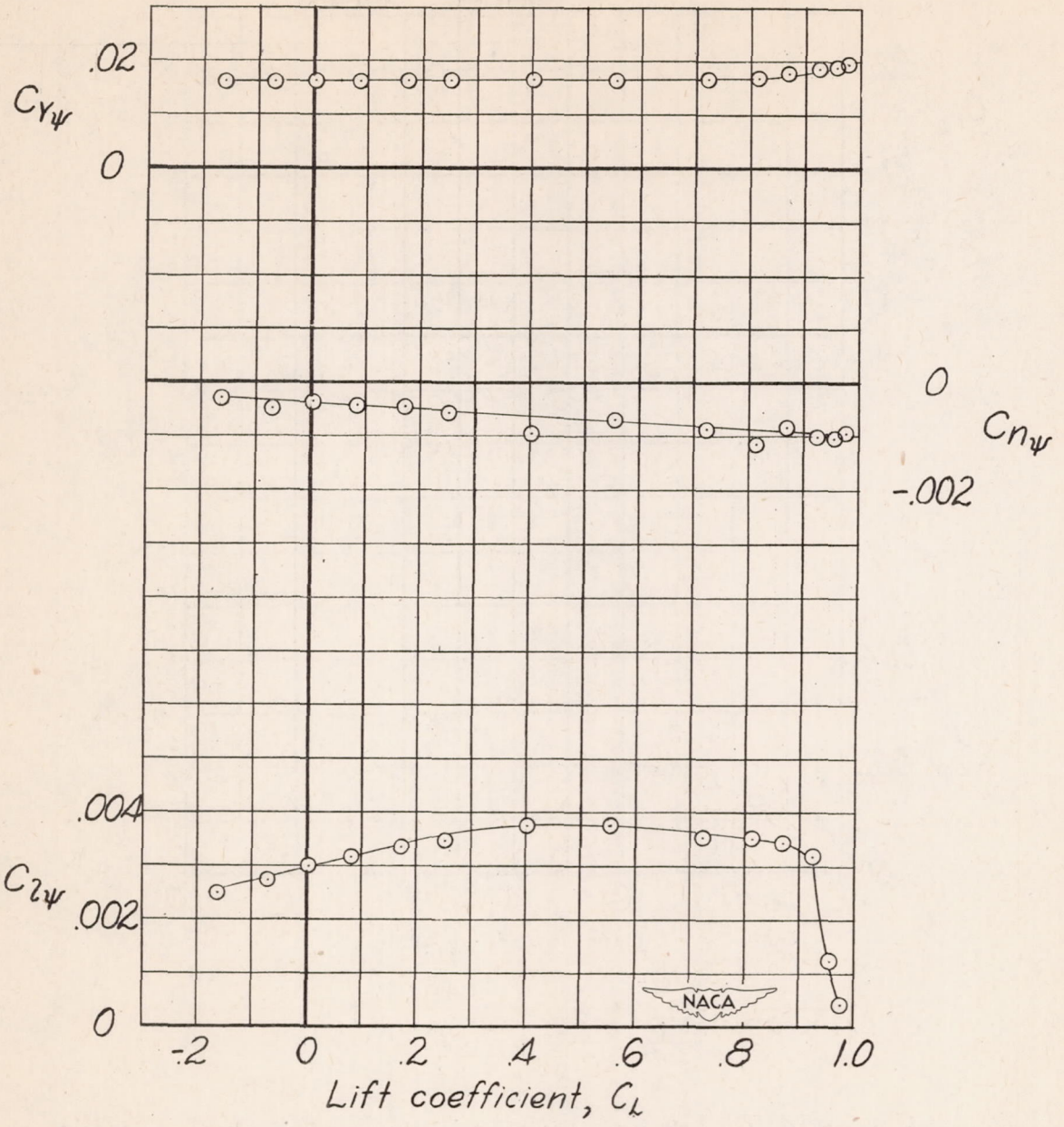

Figure 13.- The lateral-stability parameters for the basic model. Tip 1; Γ_W and $\Gamma_T = 0°$.

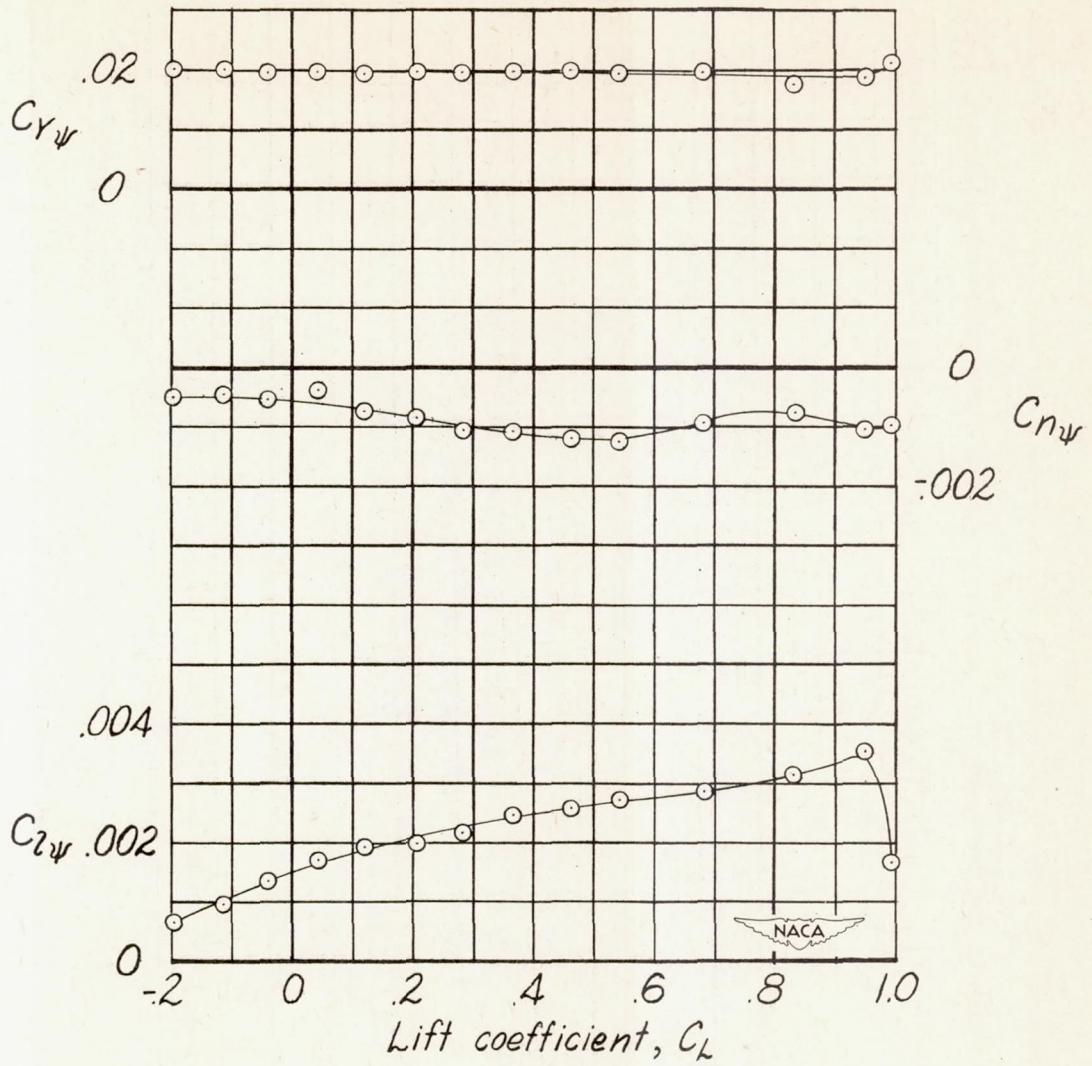

(a) Complete model.

Figure 14.- The lateral-stability parameters, $\Gamma_w = -10°$; tip 1.

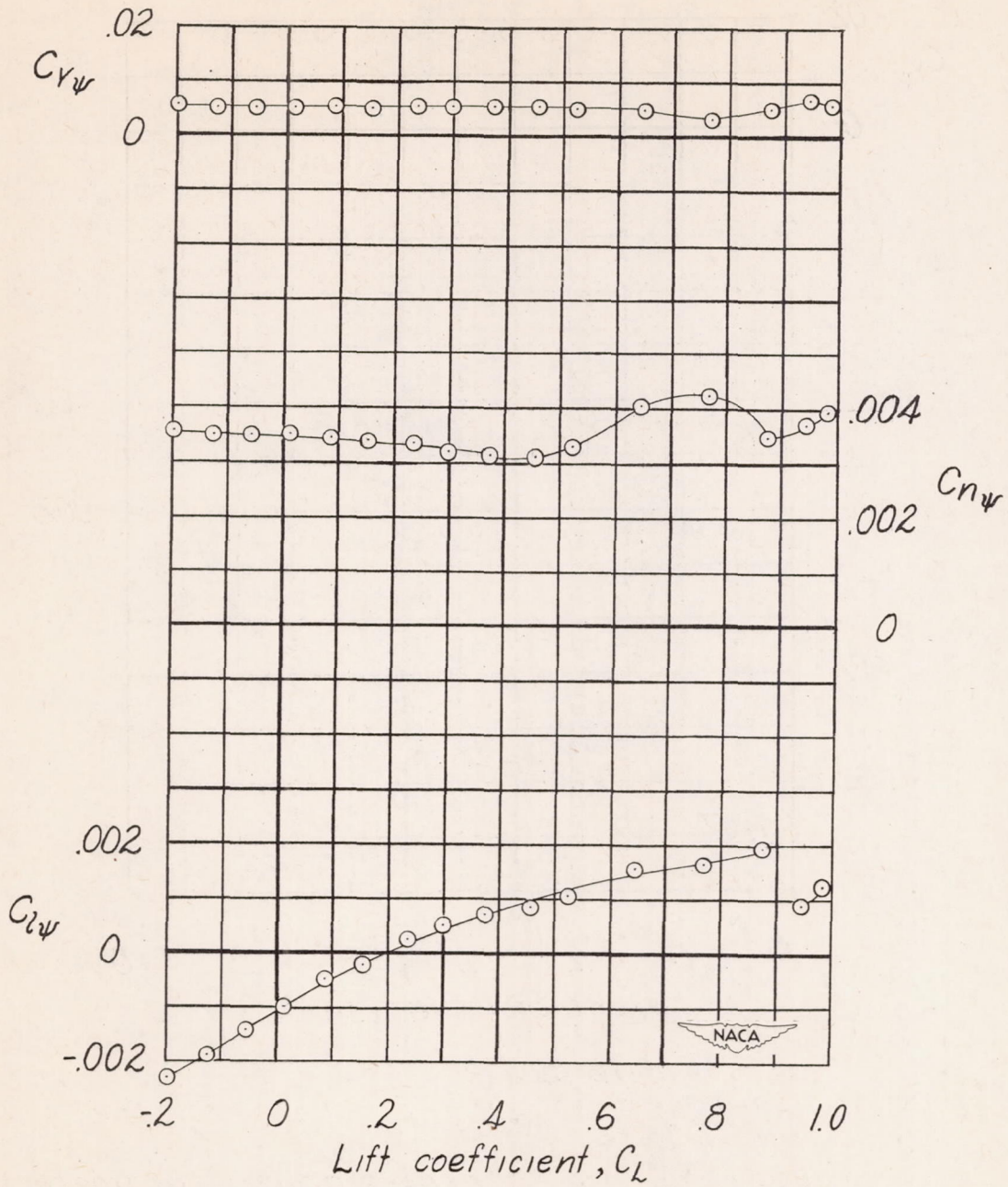

(b) Vertical and horizontal tail off.

Figure 14.- Concluded.

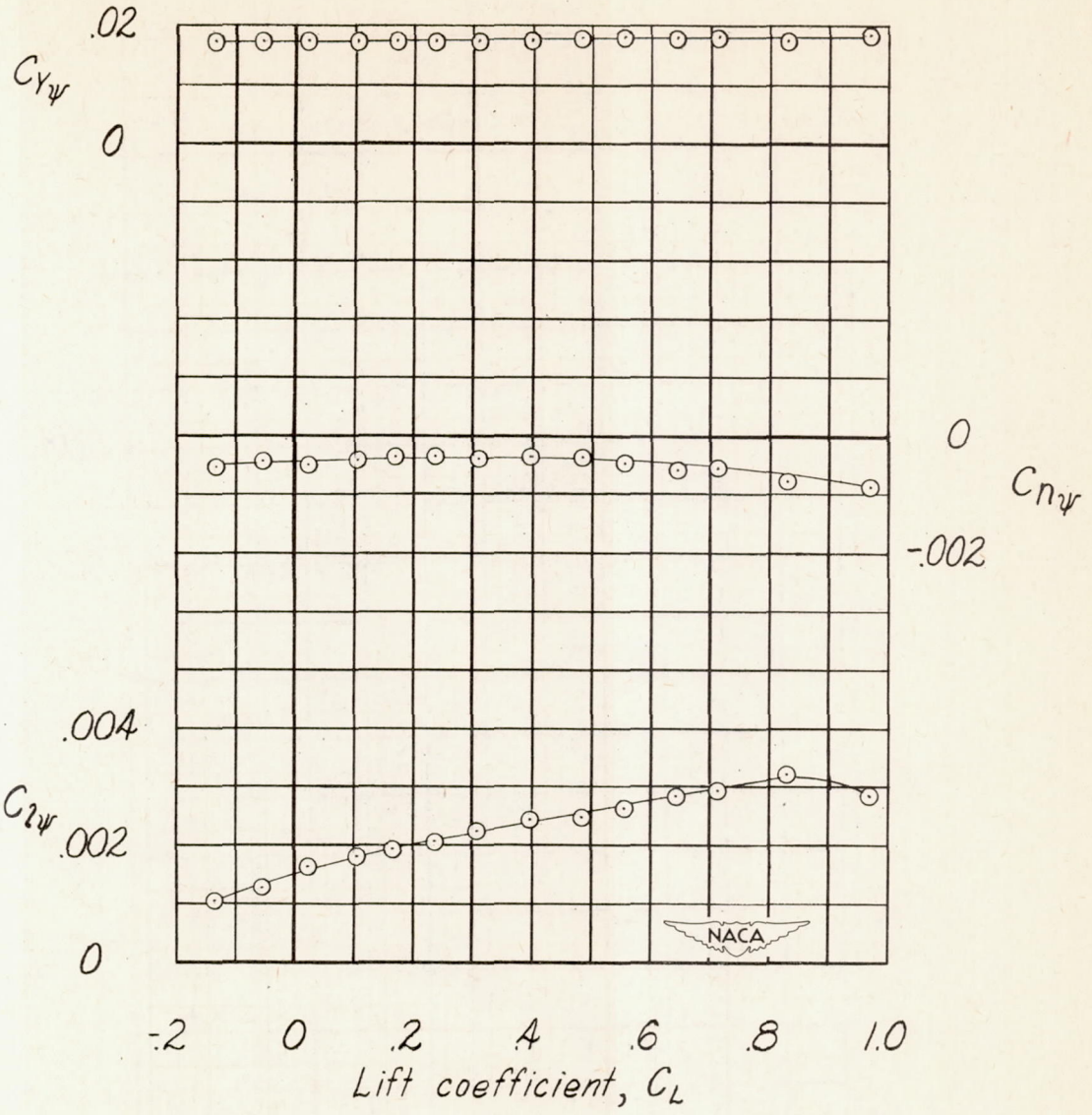

(a) Complete model.

Figure 15.- The lateral-stability parameters. $\Gamma_T = -45°$, tip 1.

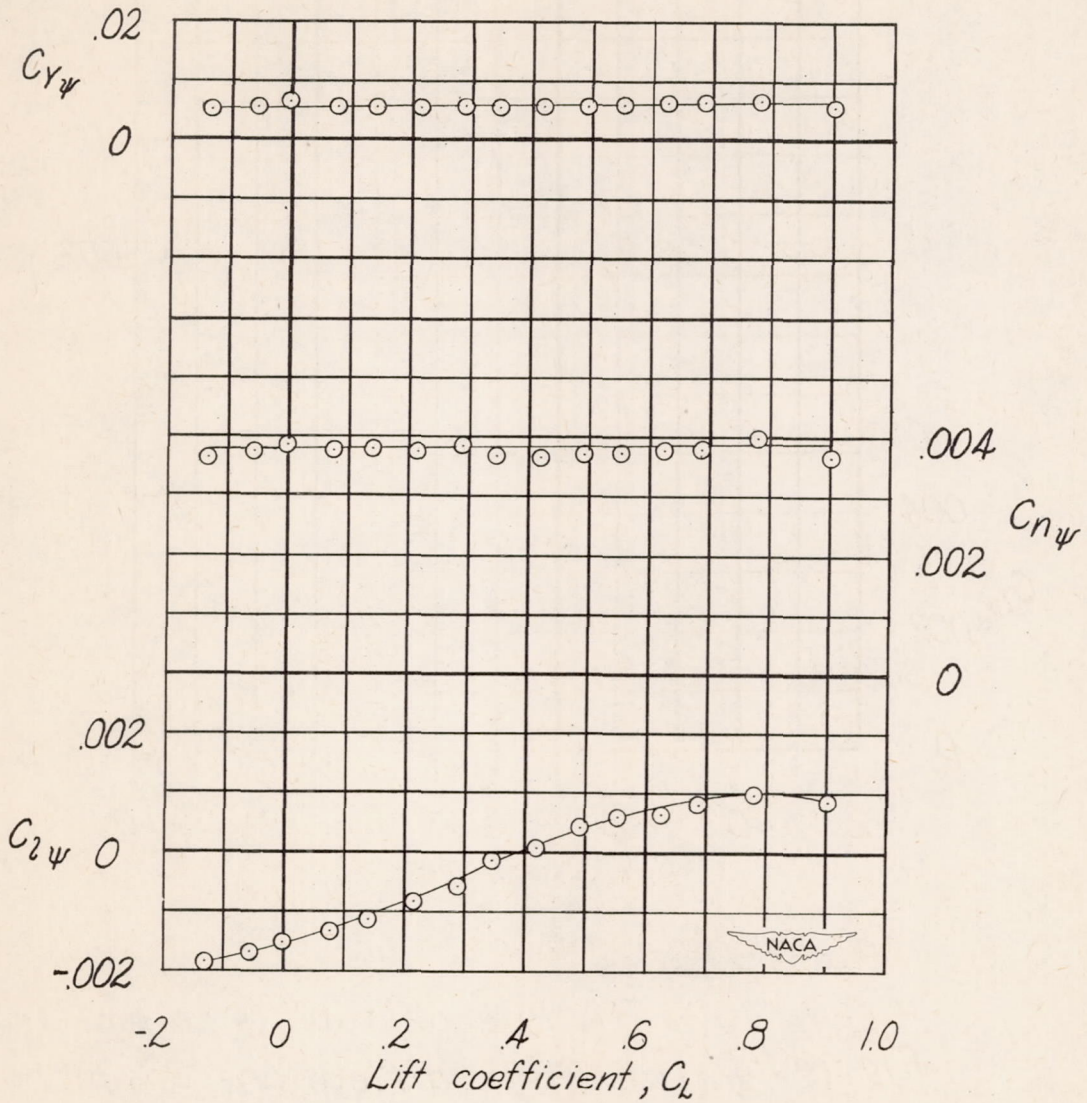

(b) Vertical and horizontal tail off.

Figure 15.- Concluded.

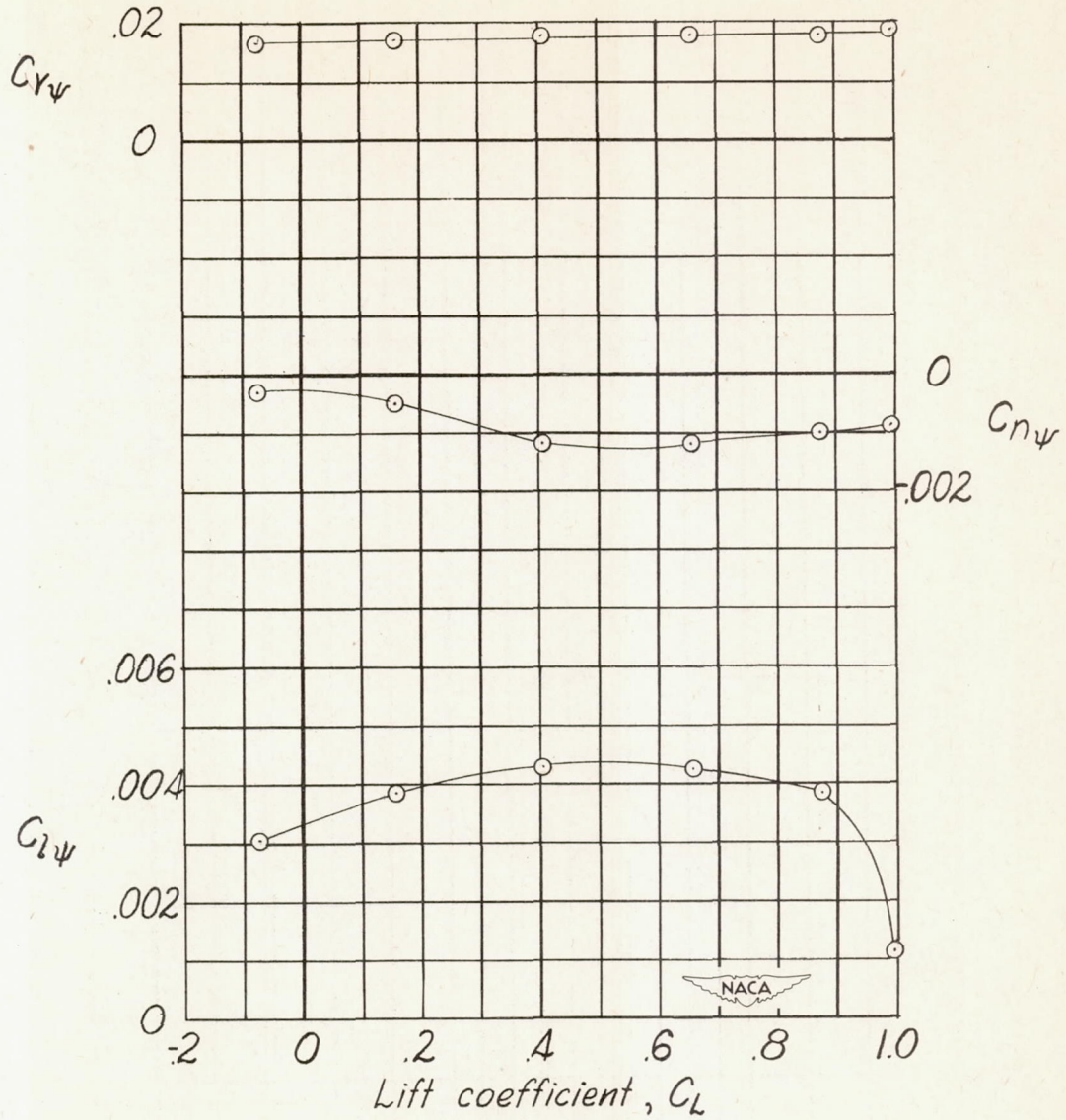

(a) Tip 1a.

Figure 16.- The lateral-stability parameters for various tip modifications. Complete model.

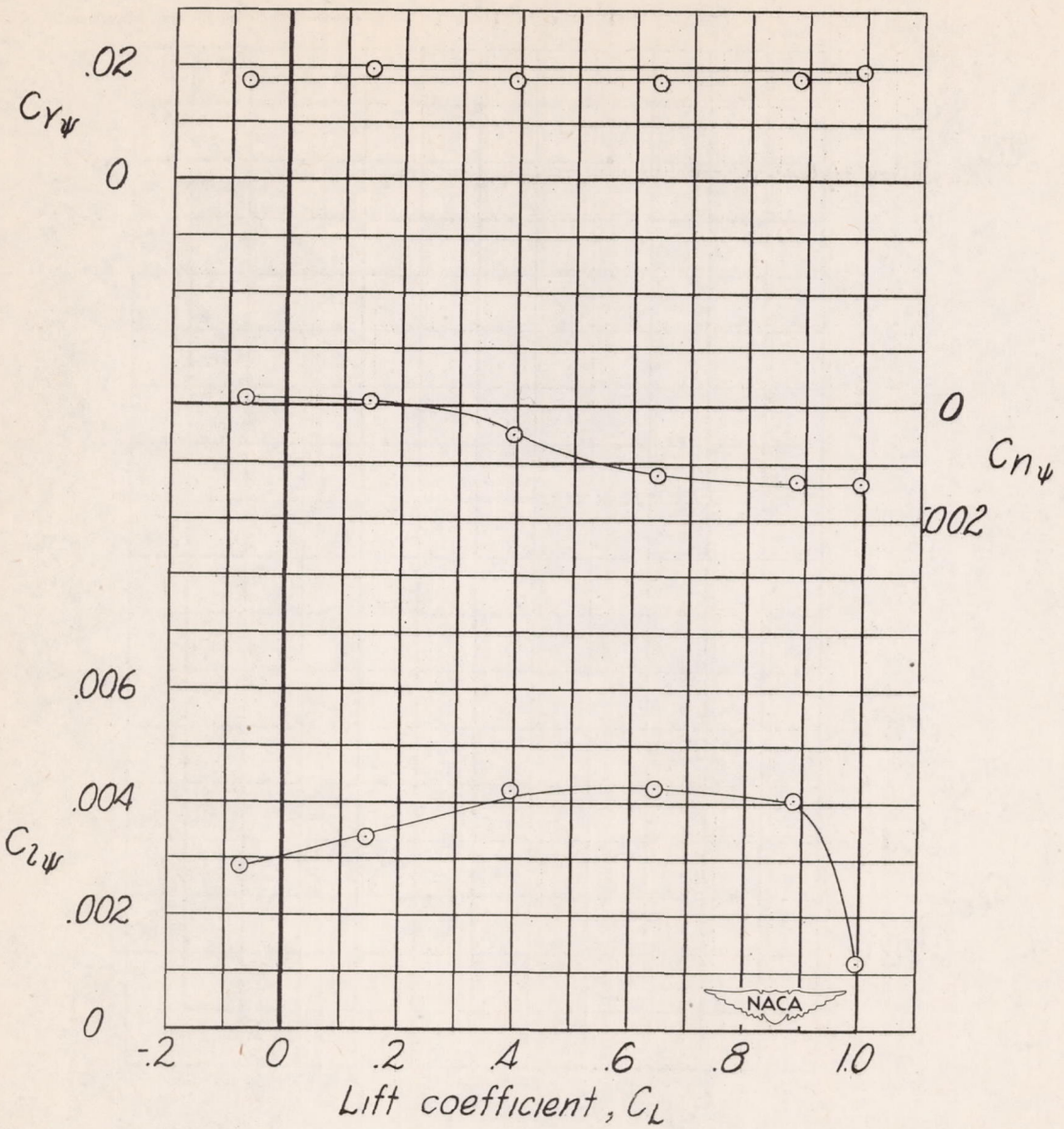

(b) Tip 2.

Figure 16.- Continued.

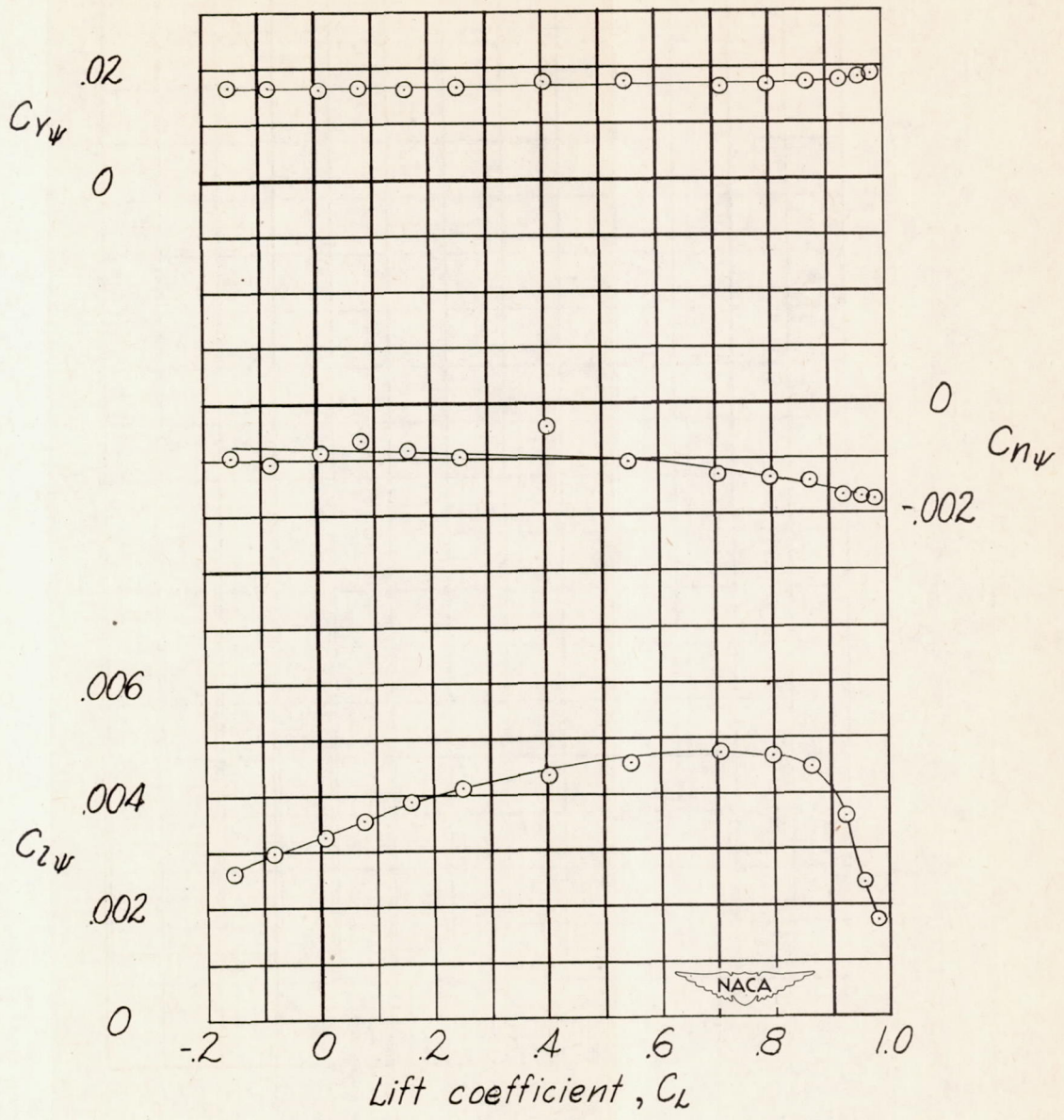

(c) Tip 3.

Figure 16.- Continued.

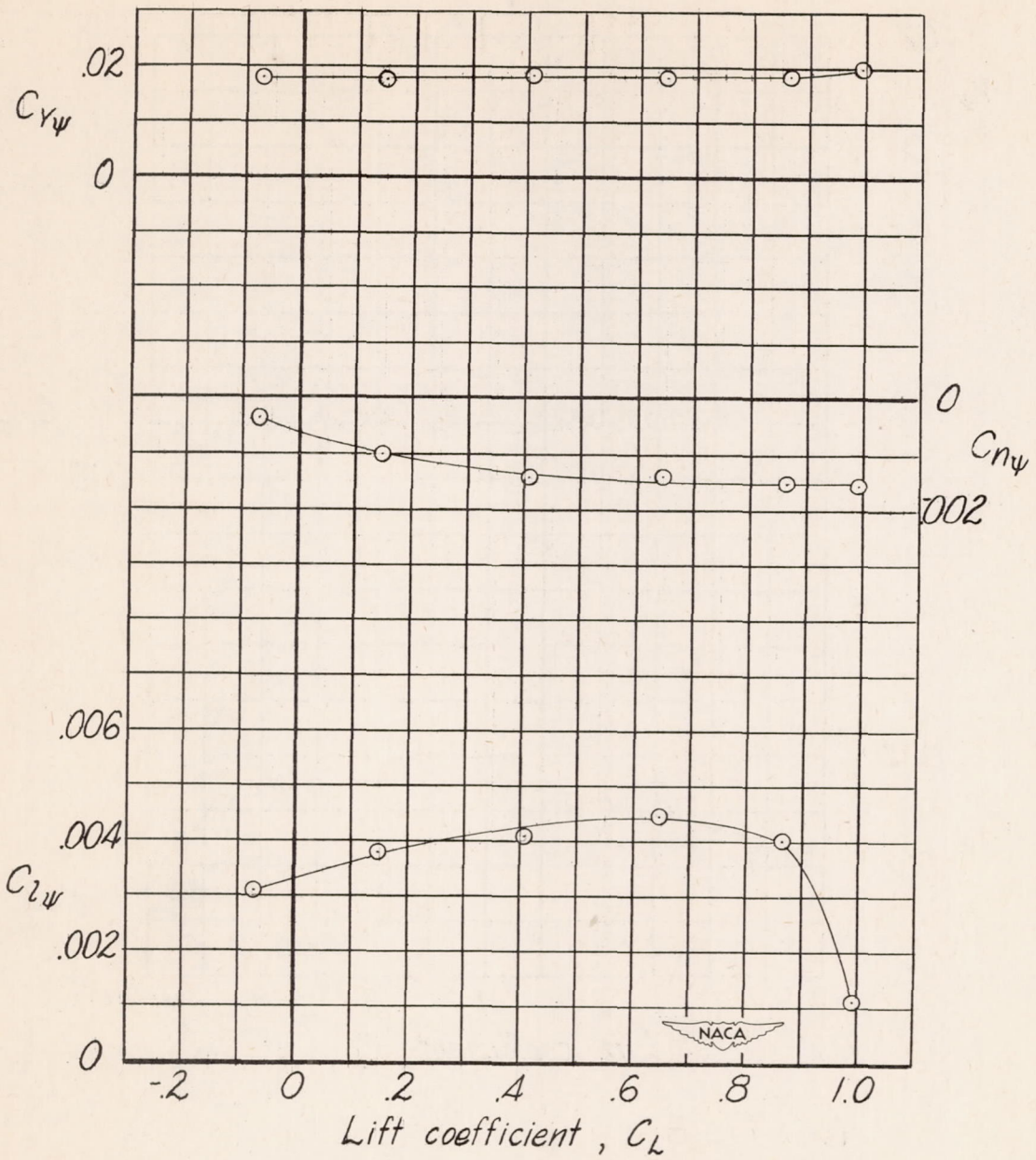

(d) Tip 4.

Figure 16.- Continued.

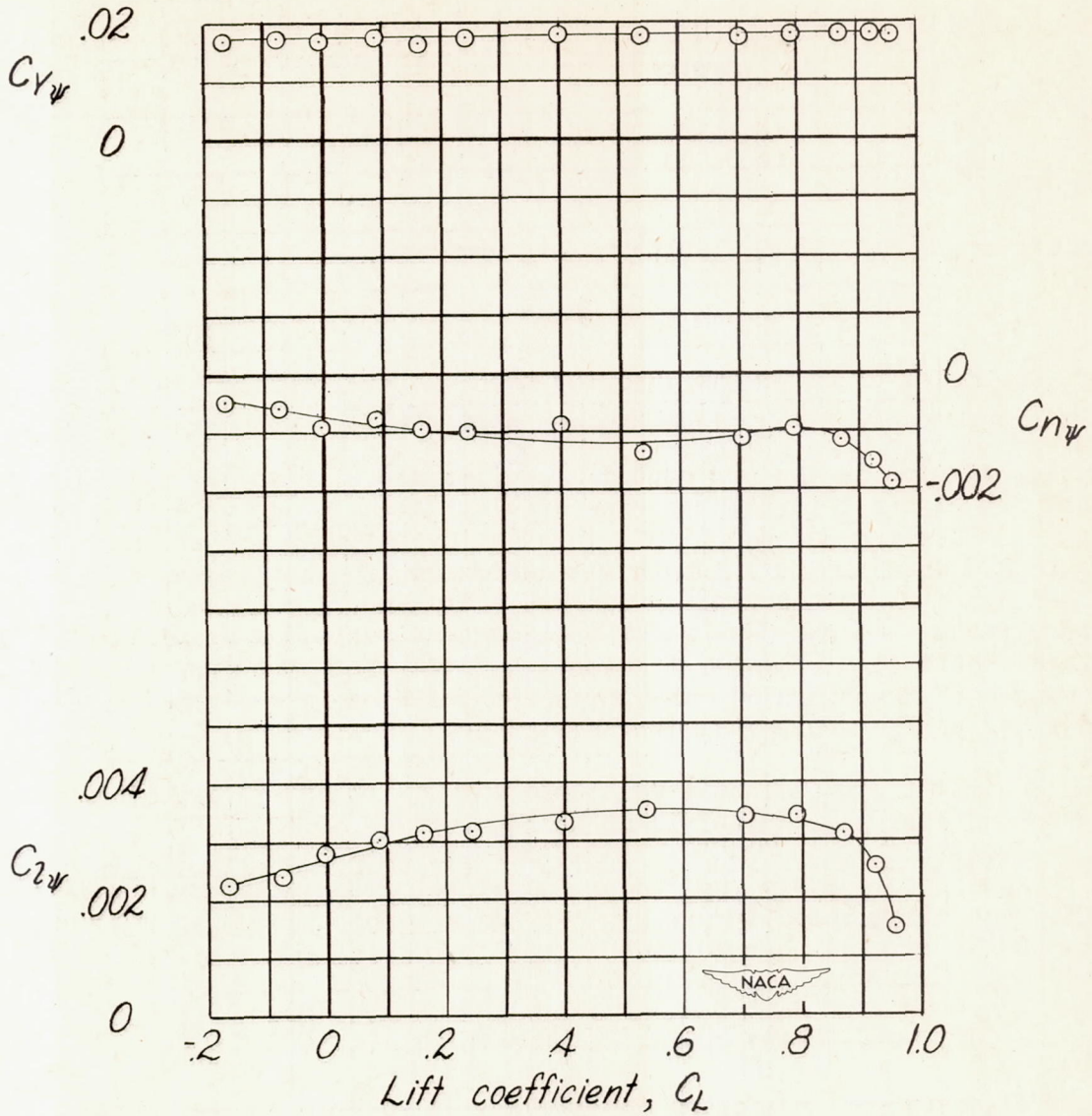

(e) Tip 5.

Figure 16.- Concluded.

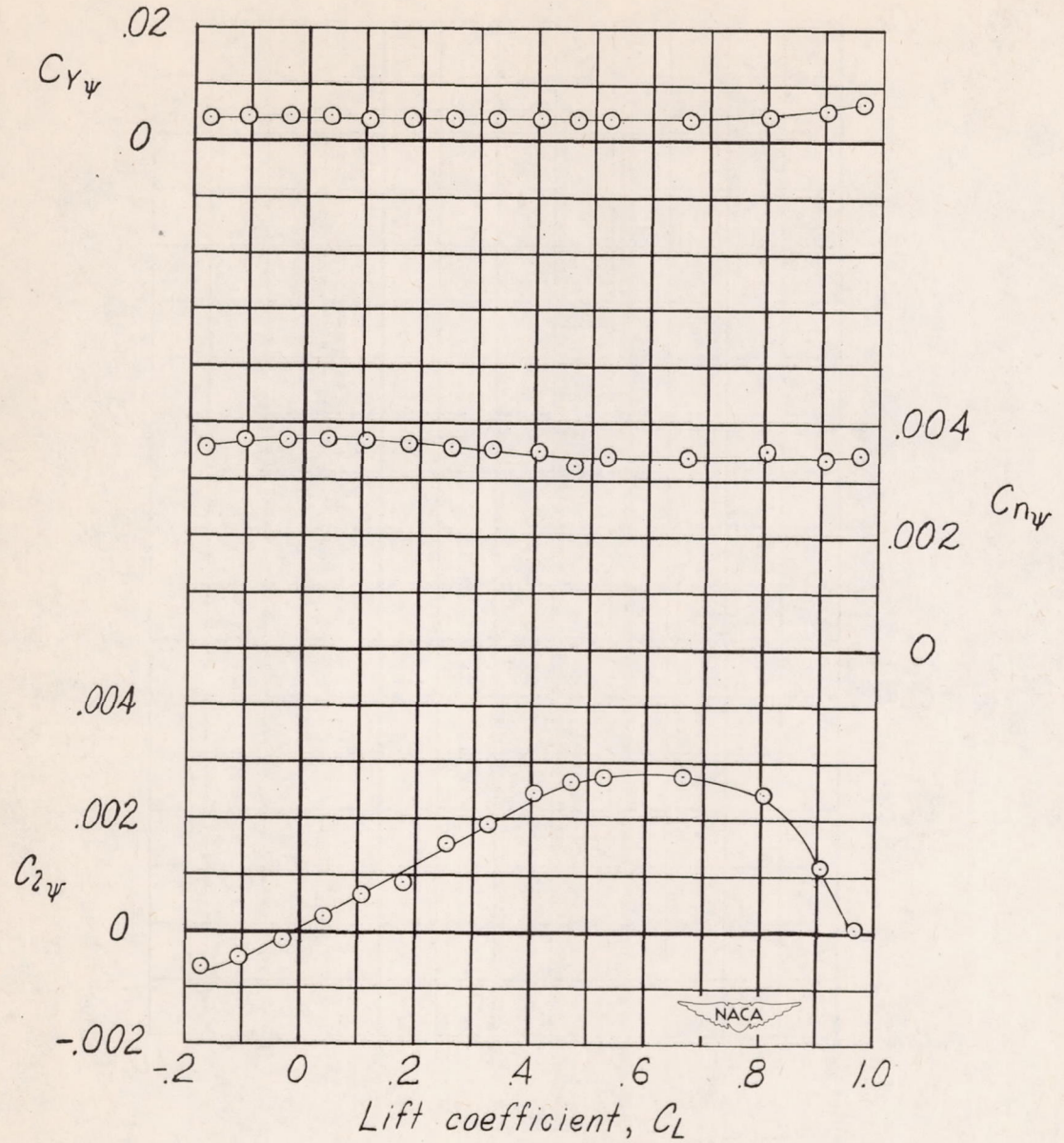

(a) Tip 1.

Figure 17.- The lateral-stability parameters for various tip modifications. Vertical and horizontal tail off.

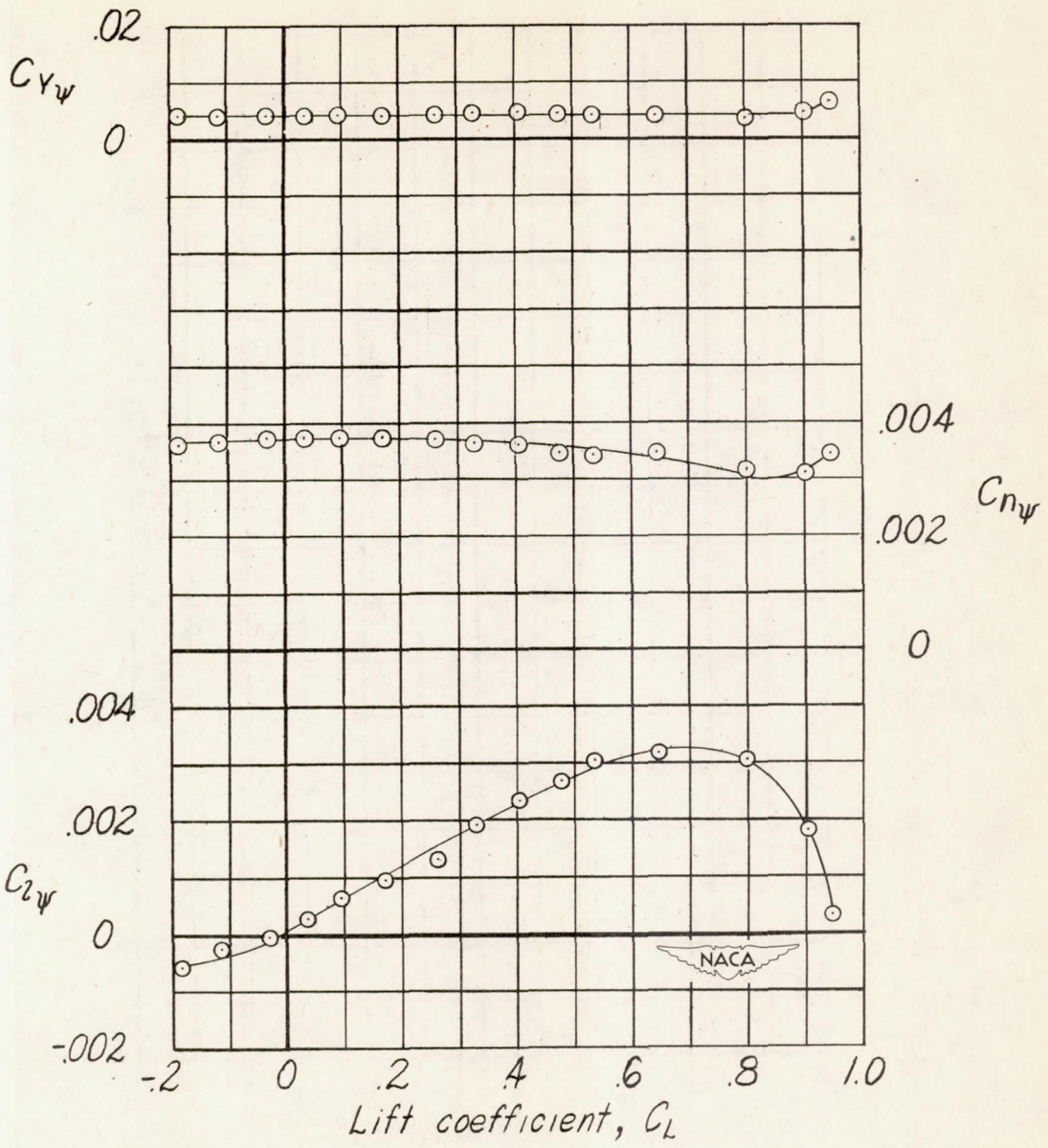

(b) Tip 3.

Figure 17.- Concluded.

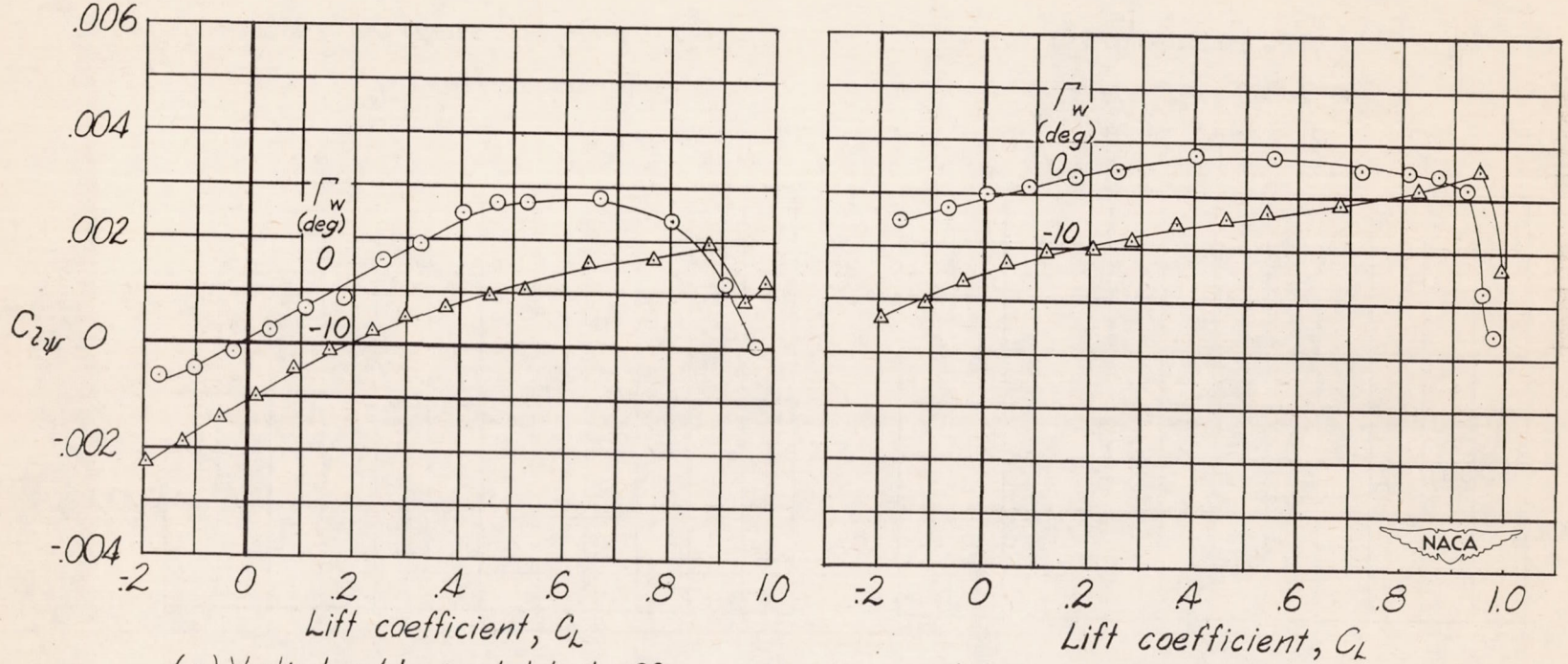

(a) Vertical and horizontal tail off.

(b) Complete model.

Figure 18.- The effect of -10° geometric dihedral on the effective-dihedral parameter. Tip 1.

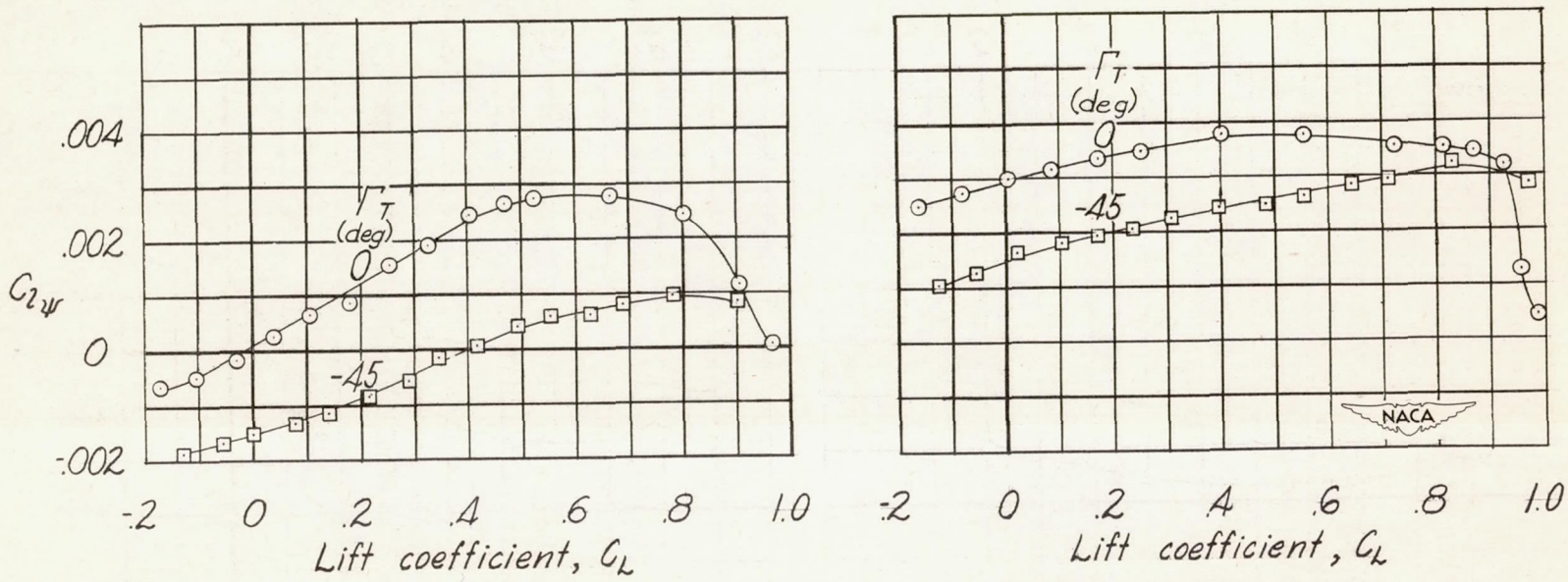

(a) Vertical and horizontal tail off.

(b) Complete model.

Figure 19.- The effect of tip droop on the effective-dihedral parameter. Tip 1.

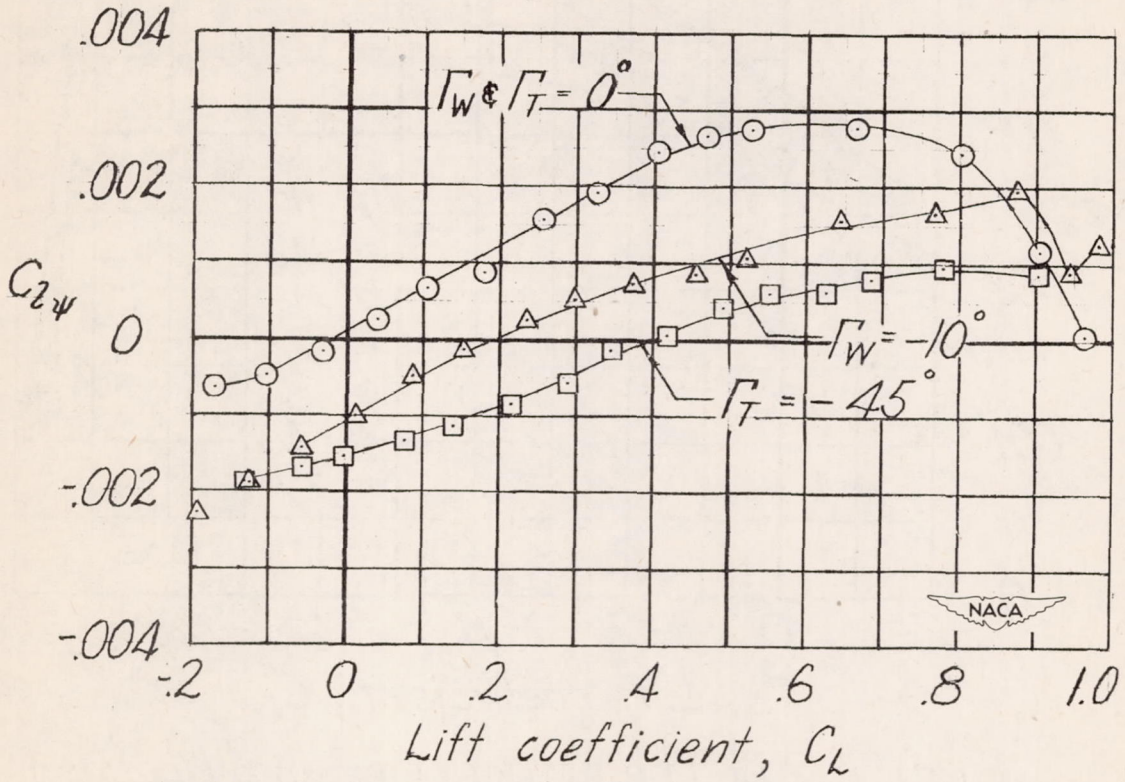

Figure 20.- Comparison of the effect of tip droop and negative geometric dihedral on the effective-dihedral parameter. Vertical and horizontal tail off.

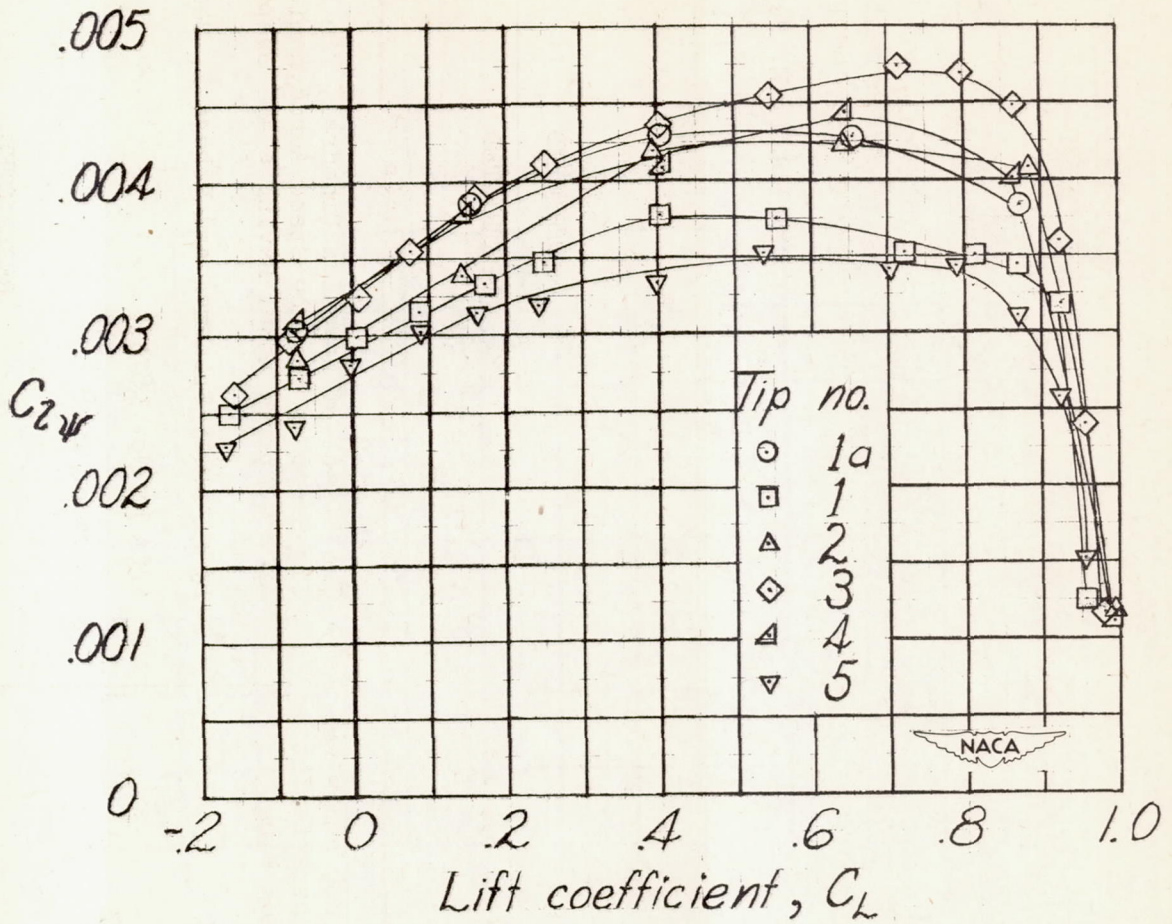

Figure 21.- The effect of tip modifications on the effective-dihedral parameter. Complete model.